



**NAVAL
POSTGRADUATE
SCHOOL**

MONTEREY, CALIFORNIA

THESIS

DEFENSE AGAINST SHIP AS A WEAPON

by

Koh Wee Yung

December 2011

Thesis Co-Advisors:

Fotis A. Papoulias

Thomas V. Huynh

Second Reader:

Khoo Boo Cheong

Approved for public release; distribution is unlimited

THIS PAGE INTENTIONALLY LEFT BLANK

REPORT DOCUMENTATION PAGE
Form Approved OMB No. 0704-0188

Public reporting burden for this collection of information is estimated to average 1 hour per response, including the time for reviewing instruction, searching existing data sources, gathering and maintaining the data needed, and completing and reviewing the collection of information. Send comments regarding this burden estimate or any other aspect of this collection of information, including suggestions for reducing this burden, to Washington Headquarters Services, Directorate for Information Operations and Reports, 1215 Jefferson Davis Highway, Suite 1204, Arlington, VA 22202-4302, and to the Office of Management and Budget, Paperwork Reduction Project (0704-0188) Washington DC 20503.

1. AGENCY USE ONLY (Leave blank)	2. REPORT DATE December 2011	3. REPORT TYPE AND DATES COVERED Master's Thesis	
4. TITLE AND SUBTITLE Defense Against Ship as a Weapon		5. FUNDING NUMBERS	
6. AUTHOR(S) Koh Wee Yung			
7. PERFORMING ORGANIZATION NAME(S) AND ADDRESS(ES) Naval Postgraduate School Monterey, CA 93943-5000		8. PERFORMING ORGANIZATION REPORT NUMBER	
9. SPONSORING /MONITORING AGENCY NAME(S) AND ADDRESS(ES) N/A		10. SPONSORING/MONITORING AGENCY REPORT NUMBER	
11. SUPPLEMENTARY NOTES The views expressed in this thesis are those of the author and do not reflect the official policy or position of the Department of Defense or the U.S. Government. IRB Protocol number _____ N/A _____.			
12a. DISTRIBUTION / AVAILABILITY STATEMENT Approved for public release; distribution is unlimited		12b. DISTRIBUTION CODE A	
13. ABSTRACT (maximum 200 words)			
<p>As an example of ships used as weapons (SAW), an oil tanker is hijacked and commandeered by terrorists to collide with a high-value maritime or shore target. If sunk or destroyed in a shipping lane as a result of a counter measure, the SAW's collateral damage would severely disrupt the traffic flow in the shipping lane. To prevent such a disruptive catastrophe, non-destructive measures must be implemented to cause the SAW to deviate from its destructive path toward the target. One such a measure involves a strategic application of forces induced by water plume barriers (WPB) to the SAW. The goal of this thesis is to examine the feasibility of realizing such a measure.</p> <p>Toward this goal, a mission analysis, using the Singapore Strait as setting and petrochemical plants on Jurong Island as targets of a SAW attack, establishes the requirement on the deviation of the SAW path from its destructive course. The nominal WPB-induced force that satisfies the deviation requirement is estimated using ship hydrostatics. Solving the equations of motion governing the response of the SAW to a strategic application of a WPB-induced force yields the SAW's motion, which is used to define a range of the WPB-induced forces and their application locations and durations that satisfy the SAW's path deviation requirement.</p> <p>Parametric studies were conducted for a range of physically realizable WPB-induced forces and application times. The results demonstrate that, in principle, the objectives of this work are achievable. These results will be validated upon the completion of an on-going research by National University of Singapore. The range of the WPB-generated forces and their application durations serve as requirements to the generation of water plume barriers.</p>			
14. SUBJECT TERMS Ship As a Weapons, Water Plume Barriers		15. NUMBER OF PAGES 85	
16. PRICE CODE			
17. SECURITY CLASSIFICATION OF REPORT Unclassified	18. SECURITY CLASSIFICATION OF THIS PAGE Unclassified	19. SECURITY CLASSIFICATION OF ABSTRACT Unclassified	20. LIMITATION OF ABSTRACT UU

NSN 7540-01-280-5500

 Standard Form 298 (Rev. 2-89)
 Prescribed by ANSI Std. Z39-18

THIS PAGE INTENTIONALLY LEFT BLANK

Approved for public release; distribution is unlimited

DEFENSE AGAINST SHIP AS A WEAPON

Koh Wee Yung
Singapore Technologies Marine
B.Eng., Nanyang Technological University, 2004

Submitted in partial fulfillment of the
requirements for the degree of

MASTER OF SCIENCE IN MECHANICAL ENGINEERING

from the

NAVAL POSTGRADUATE SCHOOL
December 2011

Author: Koh Wee Yung

Approved by: Fotis A. Papoulias
Thesis Co-Advisor

Thomas V. Huynh
Thesis Co-Advisor

Khoo Boo Cheong
Second Reader

Knox T. Millsaps
Chair, Department of Mechanical and Aerospace Engineering

THIS PAGE INTENTIONALLY LEFT BLANK

ABSTRACT

As an example of ships used as weapons (SAW), an oil tanker is hijacked and commandeered by terrorists to collide with a high-value maritime or shore target. If sunk or destroyed in a shipping lane as a result of a counter measure, the SAW's collateral damage would severely disrupt the traffic flow in the shipping lane. To prevent such a disruptive catastrophe, non-destructive measures must be implemented to cause the SAW to deviate from its destructive path toward the target. One such a measure involves a strategic application of forces induced by water plume barriers (WPB) to the SAW. The goal of this thesis is to examine the feasibility of realizing such a measure.

Toward this goal, a mission analysis, using the Singapore Strait as setting and petrochemical plants on Jurong Island as targets of a SAW attack, establishes the requirement on the deviation of the SAW path from its destructive course. The nominal WPB-induced force that satisfies the deviation requirement is estimated using ship hydrostatics. Solving the equations of motion governing the response of the SAW to a strategic application of a WPB-induced force yields the SAW's motion, which is used to define a range of the WPB-induced forces and their application locations and durations that satisfy the SAW's path deviation requirement.

Parametric studies were conducted for a range of physically realizable WPB-induced forces and application times. The results demonstrate that, in principle, the objectives of this work are achievable. These results will be validated upon the completion of an on-going research by National University of Singapore. The range of the WPB-generated forces and the application durations serve as requirements to the generation of water plume barriers.

THIS PAGE INTENTIONALLY LEFT BLANK

TABLE OF CONTENTS

I.	INTRODUCTION.....	1
	A. BACKGROUND	1
	B. RESEARCH MOTIVATION	2
	C. RESEARCH OBJECTIVE	2
	D. PROBLEM	3
	E. RESEARCH QUESTIONS	3
	F. RESEARCH SCOPE	3
	G. APPROACH TO SOLVING THE PROBLEM	4
	H. THESIS STRUCTURE	5
II.	MISSION ANALYSIS.....	7
	A. OPERATIONAL ENVIRONMENT	7
	1. Geography	7
	2. Maritime Conditions.....	8
	3. Climate and Meteorological Conditions	8
	B. POTENTIAL TARGET	9
	C. MARITIME THREAT CHARACTERISTICS.....	11
	1. Perpetrators.....	11
	2. Terrorists' Objectives	11
	3. Locations of Attacks	11
	4. Terrorists' Targets.....	12
	5. Terrorists' Tactics.....	12
	D. SCENARIO DEFINITION	13
	E. MISSION ANALYSIS RESULTS.....	16
III.	WATER PLUME BARRIER.....	17
	A. WATER PLUME BARRIER FORMATION	17
	B. WPB USED IN COUNTER-SAW MISSION.....	18
IV.	PARAMETRIC STUDY	21
	A. MATHEMATICAL FORMULATION OF SAW RESPONSE	22
	1. Equations of Motion	22
	2. Parameters	25
	3. Ship Kinematics	26
	B. NOMINAL WPB-INDUCED FORCE CALCULATION.....	26
	C. SOLUTION IMPLEMENTATION	30
	1. Calculation of Parameters.....	30
	2. MATLAB Implementation.....	31
	a. MATLAB Inputs	32
	b. MATLAB Outputs	32
V.	PARAMETRIC STUDY RESULTS AND DISCUSSION.....	35
	A. COMBINATION 1—VARIABLE MAGNITUDE OF \vec{F}_{WPB}	35

B.	COMBINATION 2—VARIABLE LOCATION OF \vec{F}_{WPB} APPLICATION.....	39
C.	COMBINATION 3—VARIABLE DURATION OF \vec{F}_{WPB} APPLICATION.....	43
VI.	PRELIMINARY ASSESSMENT	49
	A. SUMMARY OF PARAMETRIC STUDY RESULTS	50
VII.	CONCLUSION AND RECOMMENDATIONS.....	53
	A. CONCLUSION	53
	B. RECOMMENDATIONS FOR FUTURE WORK.....	54
APPENDIX A. DETERMINATION OF HYDRODYNAMIC DERIVATIVES.....		55
	1. <i>Input to Maneuvering Prediction Program (MPP1.3)</i>	55
	2. <i>Output from Maneuvering Prediction Program (MPP1.3)</i>	57
APPENDIX B. MATLAB PROGRAM CODE.....		61
LIST OF REFERENCES		65
INITIAL DISTRIBUTION LIST		67

LIST OF FIGURES

Figure 1.	Map of Singapore and Singapore Strait (From [5])	8
Figure 2.	VTIS Operational Area Sectors 1 to 9 (From [13])	10
Figure 3.	VTIS Operational Area Sector 7 to 9 (From [13]).....	10
Figure 4.	Basic ship terminology (From [16])	14
Figure 5.	The East-to-West route taken by the terrorists to attack Jurong Island (From [13]).....	15
Figure 6.	Illustration of the SAW scenario analysis (From [13]).....	16
Figure 7.	Desired WPB (From [17])	18
Figure 8.	Constructed WPB using ten bubbles (From [17]).....	18
Figure 9.	Front view of a WPB interacting on the SAW hull	19
Figure 10.	Earth-fixed coordinate system and the ship-fixed coordinate system.	22
Figure 11.	Hydrostatic force on a ship body at equilibrium.....	27
Figure 12.	Changes in the hydrostatic forces	28
Figure 13.	Plan view of the SAW and location of the applied F_{WPB}	29
Figure 14.	Time vs \dot{v}	36
Figure 15.	Time vs \dot{r}	36
Figure 16.	Time vs v	37
Figure 17.	Time vs r	38
Figure 18.	Angle of deflection vs time.....	39
Figure 19.	Time vs \dot{v}	40
Figure 20.	Time vs \dot{r}	41
Figure 21.	Time vs v	42
Figure 22.	Time vs r	42
Figure 23.	Angle of deflection vs time.....	43
Figure 24.	Time vs \dot{v}	44
Figure 25.	Time vs \dot{r}	45
Figure 26.	Time vs v	46
Figure 27.	Time vs r	46
Figure 28.	Angle of deflection vs time.....	47
Figure 29.	Input for project name.....	55
Figure 30.	Input for vessel characteristics.....	56
Figure 31.	Input for steering characteristics.....	56
Figure 32.	Input for operating conditions.....	57
Figure 33.	Input for water properties.....	57
Figure 34.	Input for run identifier	58
Figure 35.	Output from the Maneuvering Prediction Program (MPP1.3).....	59

THIS PAGE INTENTIONALLY LEFT BLANK

LIST OF TABLES

Table 1.	Example of maritime threat characteristics (From [2]).	12
Table 2.	Summary of SAW details (From [15]) and operating conditions (From [7]).	14
Table 3.	Values for F_{WPB} , location and duration of F_{WPB} application	30
Table 4.	Values of hydrodynamic derivatives	31
Table 5.	Summary of parametric study results	50

THIS PAGE INTENTIONALLY LEFT BLANK

LIST OF ACRONYMS AND ABBREVIATIONS

WPB	Water Plume Barrier
SAW	Ship as a Weapon
Bbl/d	Barrels per day
VLCC	Very Large Crude Carrier
ULCC	Ultra Large Crude Carrier
AMS	Amidships
CG	Center of Gravity

THIS PAGE INTENTIONALLY LEFT BLANK

ACKNOWLEDGMENTS

I will like to thank Dr. Fotis A. Papoulias and Dr. Tom Huynh for their guidance throughout this research. Especially, I'm grateful to Dr. Tom Huynh for going through the thesis patiently and providing invaluable comments and advice to improve it.

Most of all, I will also like to thank my wife, Bee Ping, and my son, Zach, for allowing me the time to do all the necessary work and providing support and encouragement throughout the 12 months of study at the Naval Postgraduate School.

THIS PAGE INTENTIONALLY LEFT BLANK

I. INTRODUCTION

A. BACKGROUND

This chapter discusses the increasing concerns over maritime terrorist attacks, the research motivation, and the objective of this thesis. It also defines the research scope, formulates the problem to solve in this research, discusses the approach to solving the problem, and outlines the structure of the thesis.

“A major terrorist attack that closed a port … for weeks would have severe economic consequences on world trade because it would inflict major disruptions in complex just-in-time supply chains that comprise the global economy,” the World Economic Forum said in its Global Risks 2010 report, released in January [1].

U.S. Congressional Research Service has reported to U.S. Congress that the threat of maritime terrorism is significant and takes many forms of variation and raised concerns about the possibility of maritime terrorist attacks [2]. Maritime vessels and facilities are particularly vulnerable to terrorism. Several planned seaborne attacks occurred in the past decade. Two notable events are the explosives-laden dinghy attack against the USS Cole in 2000, resulting in 17 casualties, and an attack on the Limburg in 2002, killing one crewman and spilling 90,000 barrels of oil into the Gulf of Aden [1].

Maritime terrorist attacks are not just confined to any specific region. The Straits of Malacca and Singapore between peninsular Malaysia and Sumatra can potentially attract such attacks [3]. One of the world’s busiest shipping lanes, the Straits were used by more than 70,000 ships in 2007. Up to 80% of China’s oil imports and 90% of Japan’s crude oil imports pass through the Straits [1]. They are thus vital passageways for the transportation of petroleum products from the Middle East and East Asia. The U.S. Energy Information Administration has identified the Straits as one of the world’s most strategic world oil transit chokepoints (critical parts of global energy security) [4].

If terrorists hijacked an oil tanker and used it as a weapon, hence ship as a weapon (SAW), in a successful maritime attack in the Straits, its collateral damage would disrupt the shipping lanes and the petrochemical sector in particular, thereby bringing devastation

to not only the local economies but also the global economy as well. A defensive measure is thus needed to stop the terrorists from achieving their mission. Such a defensive measure to counter the SAW, however, must not sink or destroy the SAW in a shipping lane, because its collateral damage would severely disrupt the traffic flow in the shipping lane. To prevent such a disruptive catastrophe, non-destructive measures must be implemented to cause the SAW to deviate from its destructive path toward the target. One such a measure involves a strategic application of forces induced by water plume barrier (WPB) to the SAW.

A WPB is the free water surface that is being pushed up by the bubbles created by, for example, underwater explosions. These bubbles are strategically located to create a WPB of a particular shape. The resulting WPB then exerts a force to the SAW to cause the SAW to move in a direction away from its intended destructive course. Chapter III discusses the formation of a WPB with bubbles and its interaction with the hull of the SAW.

B. RESEARCH MOTIVATION

The motivation of this research is to explore the feasibility of using a WPB as a non-destructive measure to destroy the positional stability (ship's ability to return to its original path) of a SAW aimed towards a high-value target. Such a non-destructive measure should result in neither sinking nor exploding the SAW.

C. RESEARCH OBJECTIVE

The research reported in this thesis is part of a multi-year research project. This research project is funded by National University of Singapore (NUS) for a fund of approximately SGD 400,000 over three years (2010–2013) and the Naval Postgraduate School (NPS) for a fund of USD 100,000 over a year (2010–2011). The ultimate objective of the research project is to develop and deploy a Water Plume Barrier (WPB) system to counter a SAW.

This thesis serves to initiate the research project; its objective is to assess the feasibility of applying WPB-induced forces to the hull of the SAW to alter its course and, thereby, to generate the preliminary requirements on the magnitude and sustainment of the force generated by a WPB. Specifically, it attempts to solve the problem stated in Section D.

D. PROBLEM

A SAW is commandeered by terrorists to ram a petrochemical processing plant located at the southernmost end of Jurong Island in the Singapore Strait. If sunk or destroyed as a result of a counter measure, the SAW's collateral damage would severely disrupt the traffic flow in the shipping lane. To prevent such a disruptive catastrophe, non-destructive measures must be implemented to cause the oil tanker to deviate from its destructive path toward the target. One such a measure involves a strategic application of WPB-induced forces to the SAW. The feasibility of employing the WPB measure needs to be assessed. Assessing it amounts to answering the research questions posed in Section E.

E. RESEARCH QUESTIONS

The primary research question is:

Is it feasible to use a WPB as a means to counter a SAW?

Answering this question amounts to answering the following questions:

- 1) What are the magnitudes of the WPB-induced forces required to destroy the SAW's positional stability?
- 2) Where on the hull of the SAW should the WPB-induced forces be applied?
- 3) For how long does the application of the WPB-induced forces need to be maintained?

F. RESEARCH SCOPE

The Singapore Strait is the setting, and the corresponding operational environment is considered. An oil tanker is used as a SAW and the specific target is a

petrochemical processing plant located at the southernmost end of Jurong Island. WPB optimization and simulation and WPB system design are not covered in this thesis.

G. APPROACH TO SOLVING THE PROBLEM

A three-stage approach is employed to solve the problem or to answer the questions posed in Section E. In the first stage, a mission analysis is performed. It involves (1) an analysis of the operational environment pertaining to the Singapore Strait, (2) the postulation of a potential target, (3) the identification of the threat (SAW) characteristics, (4) the definition of a specific SAW scenario, and (5) the determination of the SAW's altered path required to achieve the counter-SAW mission. The outcomes of (5) are criteria used in the assessment of the feasibility of using a WPB to counter a SAW.

In the second stage, a parametric study is conducted to determine the SAW motion resulting from responding to various combinations of the three parameters—the magnitude of the WPB-induced force, the location of its application along the hull of the SAW, and the duration of its application. This study involves formulating the mathematical problem of determining the response (including rotation and translation) of a ship exerted by a WPB-induced force, solving the resulting mathematical problem using MATLAB to obtain the SAW motion and the angles of deflection corresponding to various combinations of the three parameters. The mathematical formulation of the response involves setting up the equations of motion governing the SAW dynamics, defining initial conditions, determining the parameters in the equations of motion, such as the ship characteristics, the magnitude of the applied WPB-induced force, and the ship hydrodynamics derivatives. A computer program is used to generate the ship hydrodynamics derivatives, given the SAW characteristics and its operating environment. Various magnitudes of the applied WPB-induced forces are derived from a nominal WPB-induced force estimated using ship hydrodynamics.

In the final stage, based on the parametric study results obtained in the second stage, the requirements on the magnitude of the WPB-induced force and the duration and

the location of the application of the WPB-induced force are established for a successful counter-SAW mission.

H. THESIS STRUCTURE

This thesis consists of seven chapters. Chapter I provides the background of maritime terrorism as well as the motivation, the objective, and the scope of the research. The problem and the approach to solving the problem are also described in this chapter. Chapter II describes the mission analysis and its results, which serve as the criteria used in the assessment of the feasibility of using a WPB to counter a SAW. Chapter III discusses the formation of a WPB and its potential application in a counter-SAW mission.

Chapter IV discusses the mathematical formulation of the ship response, which involves setting up the equations of motion governing the SAW dynamics, defining initial conditions, determining the parameters in the equations of motion, such as the ship characteristics, the magnitude of the applied WPB-induced force, and the ship hydrodynamics derivatives. It also explains the calculation of the nominal WPB-induced force and demonstrates the solution implementation using MATLAB. Chapter V discusses the parametric study and its results—the effects of the magnitudes of the WPB-induced forces and the durations and the locations of the applied forces on the SAW’s orientation and kinematics. The parametric study aims to determine a combination or combinations of these three parameters that satisfy the counter-SAW mission success requirement.

Chapter VI provides a preliminary assessment of the feasibility of using a WPB to counter a SAW, in terms of the magnitude of the WPB-induced force and the duration and the location of the force for a counter-SAW mission success requirement. It summarizes the results of the different combinations of the three parameters mentioned in Chapter V.

Finally, Chapter VII recapitulates the problem and the approach to solving the problem and provides a summary of the research results and recommendations for future research.

THIS PAGE INTENTIONALLY LEFT BLANK

II. MISSION ANALYSIS

A. OPERATIONAL ENVIRONMENT

The mission analysis in this work consists of determining the operating environment pertaining to the Singapore Strait, considering a potential target, identifying the threat (SAW) characteristics, defining a specific SAW scenario, and determining the SAW's altered path required to achieve the counter-SAW mission. The SAW's altered path serves a criterion used in the assessment of the feasibility of using a WPB to counter SAW.

1. Geography

Singapore, engulfed by the Singapore Strait, is situated in the southernmost part of peninsular Malaysia and north of Indonesian Riau Islands in South East Asia. As Figure 1 shows, with the Malacca Strait in the west and the South China Sea in the east, the Singapore Strait is a 105-kilometer-long, 16-kilometer-wide strait, and it is one of the busiest waterways used by international shipping. The narrowest point of this waterway is the Phillips Channel, which is only 1.7 miles wide at its narrowest point. This creates a natural bottleneck, with the potential for a collision, grounding, or oil spill [4].



Figure 1. Map of Singapore and Singapore Strait (From [5])

2. Maritime Conditions

Surrounded by peninsular Malaysia and the islands of Indonesia, the Singapore Strait is sheltered from the harsh currents of Indian Ocean and South China Sea. The sea condition in the Singapore Strait is, therefore, relatively benign and the sea state normally does not exceed 3, corresponding to smooth wavelets with a wave height of no more than 0.5 meters [6]. The mean surface wind speed can reach up to 2.5 m/s and the average non-tidal streams are about 0.5 m/s. During monsoon seasons the tidal streams can reach up to 2.5 m/s. The surface water temperature is quite uniform, usually less than 1° C in variation and the thermal effect of the underwater current is thus minimal [7].

3. Climate and Meteorological Conditions

Singapore is located one degree north of the Equator. It has a tropical rainforest climate with no distinctive seasons, uniform temperature and pressure, high humidity, and abundant rainfall. Singapore's weather is warm and humid all year round and its average annual rainfall is around 2,340 mm [8]. However, it has four periods of monsoon

seasons—Northeast Monsoon Season (December to Early March), Inter-monsoon Period (Late March to May), Southwest Monsoon Season (June to September) and Inter-monsoon Period (October to November) [9].

B. POTENTIAL TARGET

Strategically located in the Straits of Malacca and Singapore, Singapore is the world's busiest port and is the largest transshipment hub. The Singapore Strait is its lifeline for trade, food supply, and other material needs [10].

Singapore is also one of the world's top petrochemical hubs. This reputation is achieved with the development of Jurong Island into a premier petrochemical hub that hosts over 95 global companies, including Shell, ExxonMobil, Chevron, DuPont™, BASF, Sumitomo Chemicals, and Mitsui Chemicals. Jurong Island has drawn cumulative fixed asset investments of over S\$30 billion and employed about 8,000 employees [11]. The petrochemical sector has contributed almost 5% of Singapore's gross domestic product in 2007 [12]. In addition, Singapore is the world's top three oil refining centers. Jurong Island is not just important to Singapore; it is also critical to the world oil trade.

The Straits of Malacca and Singapore are divided in to nine sectors by Singapore's Vessel Traffic Information System (VTIS), operated by Maritime Port Authority (MPA). Figure 2 shows the VTIS Operational Area Sectors 1 to 9, starting from Port Klang to Singapore Strait leading to the South China Sea. Figure 3 shows a close-up of Sectors 7 to 9 in the Singapore Strait.

With its close proximity and accessibility to the Strait of Singapore, Jurong Island is a high-value target to terrorists, because a successful attack on Jurong Island would cause major economic and energy disruption to the world economy.

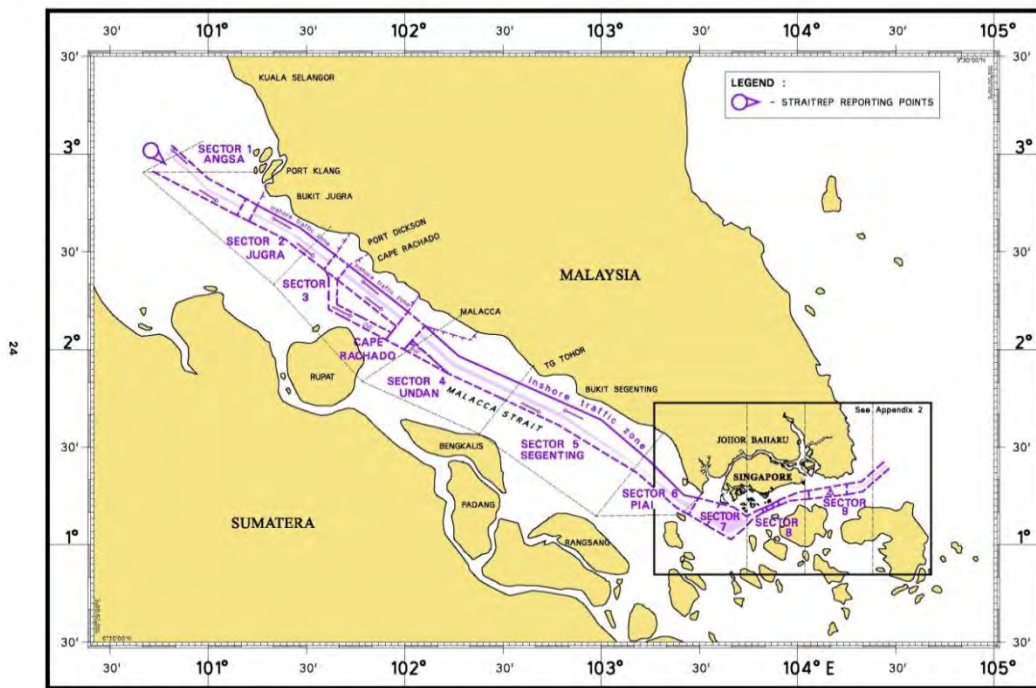


Figure 2. VTIS Operational Area Sectors 1 to 9 (From [13])

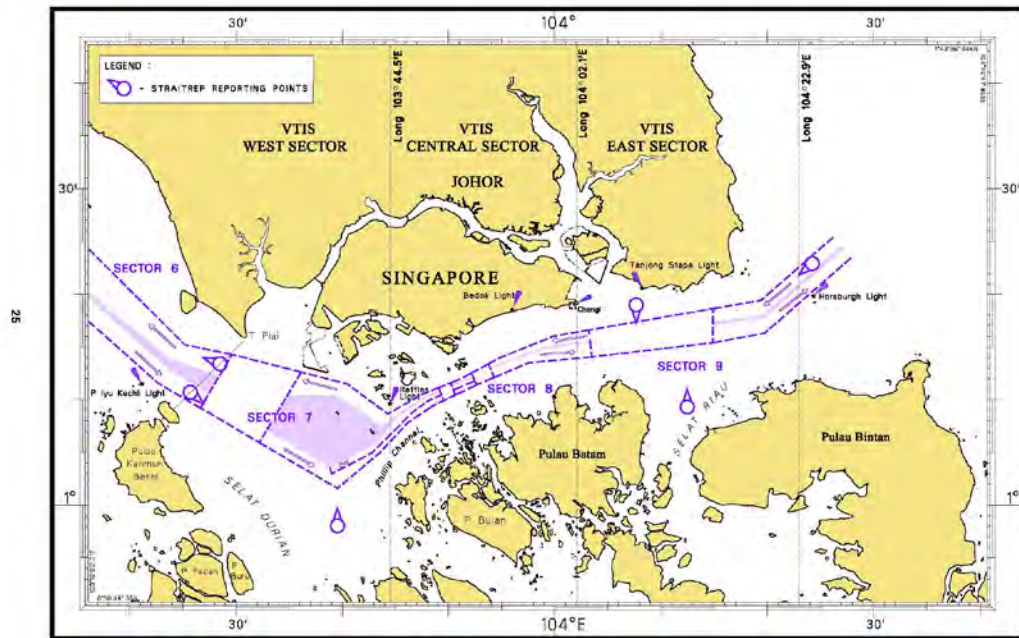


Figure 3. VTIS Operational Area Sector 7 to 9 (From [13])

C. MARITIME THREAT CHARACTERISTICS

The information in this section comes from CRS Report for Congress [2]. The threat of maritime terrorism is significant and varies with attack scenarios. These scenarios can be categorized according to five common dimensions: perpetrators, objectives, locations, targets, and tactics. These dimensions are useful for discussing historical instances of maritime terrorism and for defining potential scenarios for future maritime attacks. Table 1 can aid in generating numerous scenarios based on different combinations of the dimensions.

1. Perpetrators

It is important to identify potential perpetrators for evaluating maritime attacks as the perpetrators' backgrounds and capabilities will bear on the types of attacks. For example, terrorists who are trained in seamanship may use this skill to ram a SAW to its target. In the SAW case, the perpetrators are thus the terrorists.

2. Terrorists' Objectives

The objectives of maritime terrorism can vary—from causing human casualties to economic losses or other negative impacts. The consequences of a maritime terrorism attack can be minor or major. If human casualties are the primary objective, the potential targets are likely to be passenger/cruise ships. If economic loss is the principal objective, terrorists will likely pick containers ships, oil tankers, or ship channels as targets so as to disrupt shipping or trading. The attack on Limburg was of such an objective; it caused a reduction in Yemeni shipping volume by 50% and increased shipping insurance premium by 300%. Also, an undesirable impact of the Limburg attack was the spilling of 90,000 barrels of oil, causing environmental damage [1].

3. Locations of Attacks

Terrorist attacks on vessels are likely to occur in areas of high shipping activities, especially in ports or at shipping chokepoints, such as the Straits of Malacca and Singapore.

4. Terrorists' Targets

A potential target for a SAW can be an oil tanker, a port, or a shore-based petrochemical plant.

5. Terrorists' Tactics

In a maritime terrorism attack, terrorists can employ simple and yet effective tactics such as ramming a maritime target with an explosives-laden dinghy. As aforementioned, the USS Cole and Limburg attacks demonstrated the effectiveness of such a tactic. A more complex tactic is to hijack a large vessel, in particular a vessel with petroleum/chemical cargo, and ram it to another high-value vessel or a critical shore-based target; the petroleum/chemical cargo serves as the explosive component of the attack.

Table 1. Example of maritime threat characteristics (From [2])

Dimensions	Example Characteristics
Perpetrators	<ul style="list-style-type: none">• Al Qaeda and affiliates• Islamist unaffiliated• Foreign nationalists• Disgruntled employees• Others
Objectives	<ul style="list-style-type: none">• Mass casualties• Port disruption• Trade disruption• Environmental damage
Locations	<ul style="list-style-type: none">• Shipping chokepoints• Ports• Shore based petrochemical processing infrastructure
Targets	<ul style="list-style-type: none">• Military vessels• Cargo vessels• Fuel tankers• Ferries / cruise ships• Port area populations

Dimensions	Example Characteristics
	<ul style="list-style-type: none"> • Ship channels • Port industrial plants • Offshore platforms
Tactics	<ul style="list-style-type: none"> • Explosives in suicide boats • Explosives in light aircraft • Ramming with vessels • Ship-launched missiles • Harbor mines • Underwater swimmers • Unmanned submarine bombs • Exploding fuel tankers • Explosives in cargo ships • WMDs in cargo ships

D. SCENARIO DEFINITION

The scenario defined in this research is now described. A group of terrorists, whose objective is to disrupt the global oil trade by destroying one of the shore-based petrochemical processing plants located at the southernmost end of Jurong Island, hijacks Ocean Jewel [15], an oil tanker on its westbound shipping course in Sector 7 of the Singapore Strait (Figure 5). As the hijacked vessel reaches the point at the shortest distance to the targeted plant, the terrorists maneuver it into an abrupt right turn to head towards the plant at full speed with the intent to ram it to the plant, exploiting its cargo of petroleum product as the explosive component in order to magnify the damage that the attack can inflict. The oil tanker in the hands of the terrorists has thus become a SAW.

Based on Table 2, which shows both the SAW (Ocean Jewel) details and the operating conditions for the scenario, the SAW attack begins at 4 km from its intended target, and the estimated time of SAW collision with its intended target is 5 minutes. The ship terminology used in Table 2 is explained in Figure 4. The length overall (LOA) refers to the distance between the ship extremities. The length between perpendiculars (LBP) is the distance between the after and forward perpendiculars, measured parallel to the load line [14]. The length at the waterline (LWL) is the distance from the forward

most point of the waterline measured in profile to the stern-most point of the waterline. The beam is the breadth of a ship at the widest point. The depth is the vertical distance from the lowest point of the hull to the deck level. The draft is the vertical distance from the lowest point of the hull to the water level. The freeboard is the difference between the depth and the draft.

Table 2. Summary of SAW details (From [15]) and operating conditions (From [7])

SAW Characteristics:	Vessel Type	Crude oil tanker
	Length between perpendiculars - LBP (m)	265
	Beam (m)	43.2
	Depth (m)	23.8
	Draft (m)	17.38
	Full Speed (kts)	25
	Full Speed (m/s)	12.86
Operating Conditions:	Sea State	< 2 (calm rippled sea with a wave height no more than 0.1 meters)
	Density of Seawater (kg/m ³)	1025
	Gravitational acceleration (m/s ²)	9.81

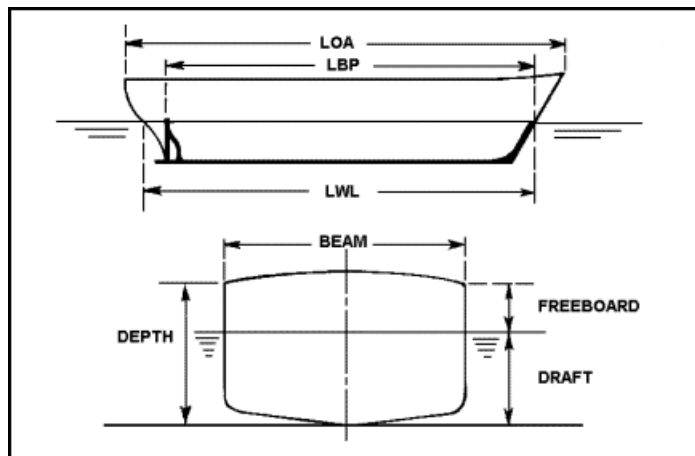


Figure 4. Basic ship terminology (From [16])

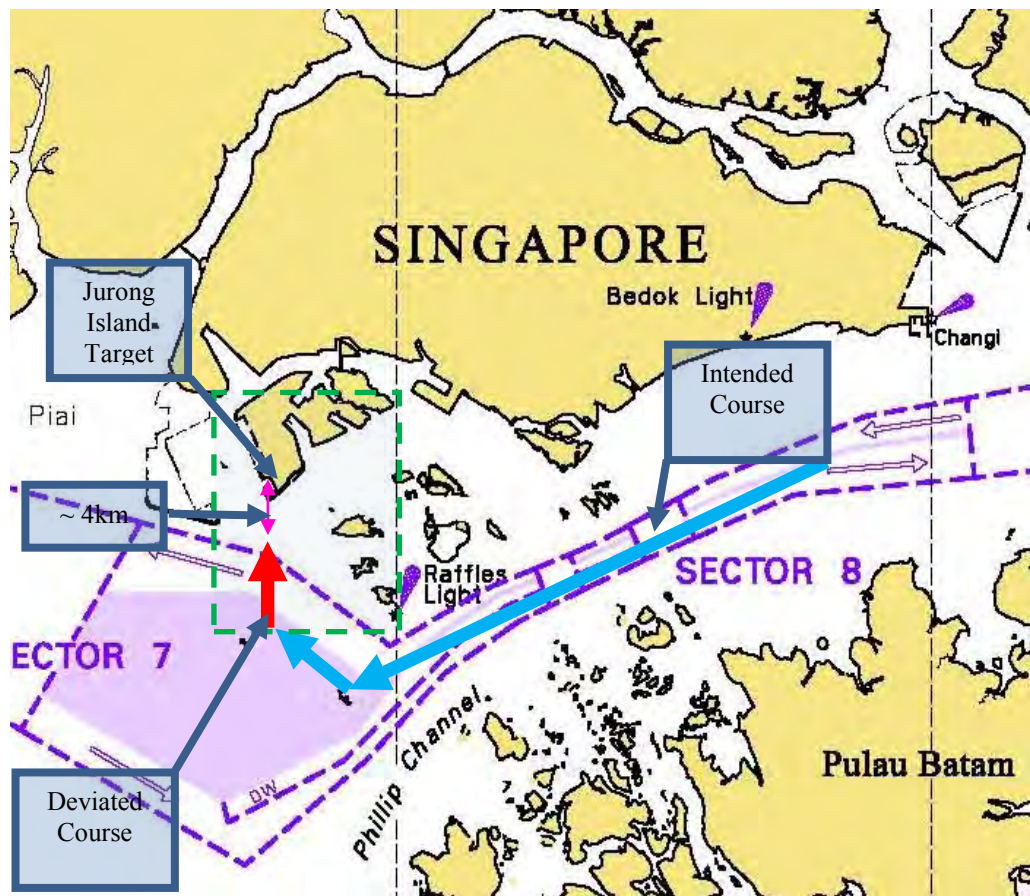


Figure 5. The East-to-West route taken by the terrorists to attack Jurong Island (From [13])

In regards to the counter-SAW operational aspect of the scenario, the following assumptions are made:

- A WPB is applied only once.
- The SAW does not maneuver to counter the effects of the WPB application.
- The duration of an effective WPB application is as small as possible so as to minimize the burden on WPB generation.

The SAW's destructive course must be altered as early as possible and a quickly as possible after the WPB application.

E. MISSION ANALYSIS RESULTS

There are various ways to neutralize the SAW in the above SAW scenario. But, as aforementioned, an operational requirement is that a measure to counter the SAW must not sink or destroy the SAW. A measure that satisfies this requirement is to divert the SAW from its destructive course toward its targeted plant on Jurong Island.

In Figure 6, the red line indicates the SAW destructive course toward its targeted plant. The green lines indicate the off-collision course required to steer clear of the target to either port (left) or starboard (right) side of the SAW. With the standoff distance of four kilometers, a deflection angle of 30° is thus required.



Figure 6. Illustration of the SAW scenario analysis (From [13])

III. WATER PLUME BARRIER

This chapter discusses the formation of a water plume barrier (WPB) and its potential application in a counter-SAW mission.

A. WATER PLUME BARRIER FORMATION

A WPB is the free water surface that is being pushed up by the bubbles created by, for example, underwater explosions. A set of bubbles initiated under high pressure will oscillate and eventually collapse asymmetrically with the water jet directed away from the initial quiescent free surface [17]. As a result, a WPB is formed.

It is of interest to create in a short time a WPB shape with a determined series of distributed bubbles created by underwater explosions. Certain functionality requires certain shape of the water plume barrier. A desired shape can be obtained with the right values of the bubble parameters, such as lateral positions, depths, and strengths. To simplify the optimization of the bubble parameters, the Proper Orthogonal Decomposition (POD) is used [17]. In this approach, a set of solution snapshots of the bubble and free surface interaction problem are used to form a set of linear POD basis functions, which, together with their POD coefficients, are then used to optimize the bubble parameters in order to attain the desired WPB shape. A detailed discussion of the use of the POD method to optimize the bubble parameters can be found in [17].

As an example, a desired 3-D WPB is shown in Figure 7. The 3-D WPB pertaining to 10 distributed underwater explosion bubbles, shown in Figure 8, is created using the POD approach. This approach is efficient; achieving this 3-D WPB takes 50 seconds on a Intel Xeon 2.8GHz processor, RAM 2.0Gb [17].

The next section discusses the use of a WPB in a counter-SAW mission.

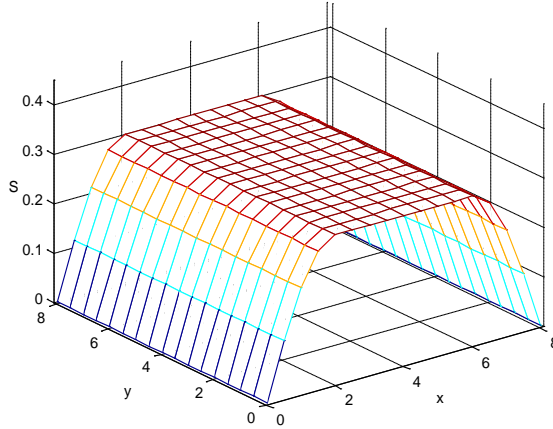


Figure 7. Desired WPB (From [17])

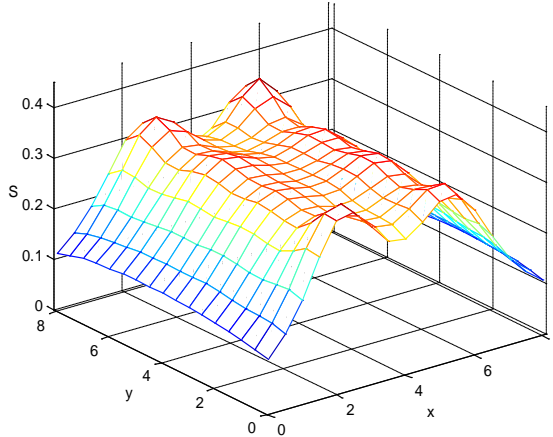


Figure 8. Constructed WPB using ten bubbles (From [17])

B. WPB USED IN COUNTER-SAW MISSION

A set of underwater bubbles created by underwater explosions can lead to the formation of a water plume in the sea surface. These bubbles are strategically located to create a particular shape WPB to alter the SAW destructive course in the yaw direction. Figure 9 illustrates a set of underwater bubbles which forms the WPB and the interaction between the WPB and the SAW hull.

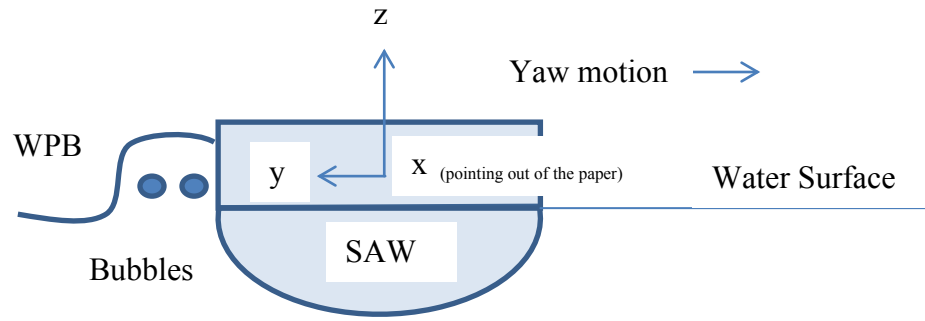


Figure 9. Front view of a WPB interacting on the SAW hull

The WPB induces a force on the SAW hull, and this WPB-induced force needs to be of a certain minimum magnitude and the duration of its application needs to be sufficient long in order to steer the SAW clear off its destructive course (a deflection angle of 30° as stated in Section E of Chapter II). Chapter VI elaborates the minimum magnitude of the force required and the duration and location of application of the force.

THIS PAGE INTENTIONALLY LEFT BLANK

IV. PARAMETRIC STUDY

As discussed in Chapter I, three parameters to be determined in countering a SAW are: the magnitude of the WPB-induced force, the location of its application along the hull of the SAW, and the duration of its application. As discussed in Chapter II, a successful counter-SAW mission requires that, at a standoff distance of four kilometers from its targeted plant on Jurong Island, the SAW be steered by 30° to either its port (left) or starboard (right) side off its destructive course toward its target. The objective of the parametric study conducted in this research is to determine a combination or combinations of these three parameters that satisfy the counter-SAW mission success requirement.

This chapter captures the parametric study. It involves generating the mathematical problem of determining the response (including rotation and translation) of a ship exerted by a WPB-induced force and solving the resulting mathematical problem, using MATLAB to obtain the SAW motion and the angles of deflection corresponding to various combinations of the three parameters. The formulation of the mathematical problem of determining the response involves setting up the equations of motion governing the SAW dynamics, defining initial conditions, determining the parameters in the equations of motion, such as the ship characteristics, the magnitude of the applied WPB-induced force, and the ship hydrodynamics derivatives. A computer program is used to generate the ship hydrodynamics derivatives, given the SAW characteristics and its operating environment. Various magnitudes of the applied WPB-induced forces are derived from a nominal WPB-induced force, which is estimated using ship hydrodynamics.

The input to this parametric study is tied to the parameters in the equations of motion. These parameters are divided into two groups: fixed parameters and variable parameters. The fixed parameters are the ship characteristics and the ship hydrodynamics derivatives. The variable parameters are the magnitudes of the applied WPB-induced forces, the durations of their applications, and the locations of their applications along the hull of the SAW.

The output of this parametric study consists of the temporal evolution of the SAW translational and rotational variables and the deflection angle of the SAW path for various combinations of the magnitude of the WPB-induced force, the location of its application along the hull of the SAW, and the duration of its application of the WPB-induced force.

A. MATHEMATICAL FORMULATION OF SAW RESPONSE

1. Equations of Motion

Two coordinate systems are used: the earth-fixed coordinate system and the ship-fixed coordinate system (Figure 10). The x_0 -axis, y_0 -axis, and z_0 -axis of the earth-fixed coordinate system form a right-handed coordinate system. The x -axis, y -axis, and z -axis of the ship-fixed coordinate system, whose origin is at the amidships (AMS), form a right-handed coordinate system.

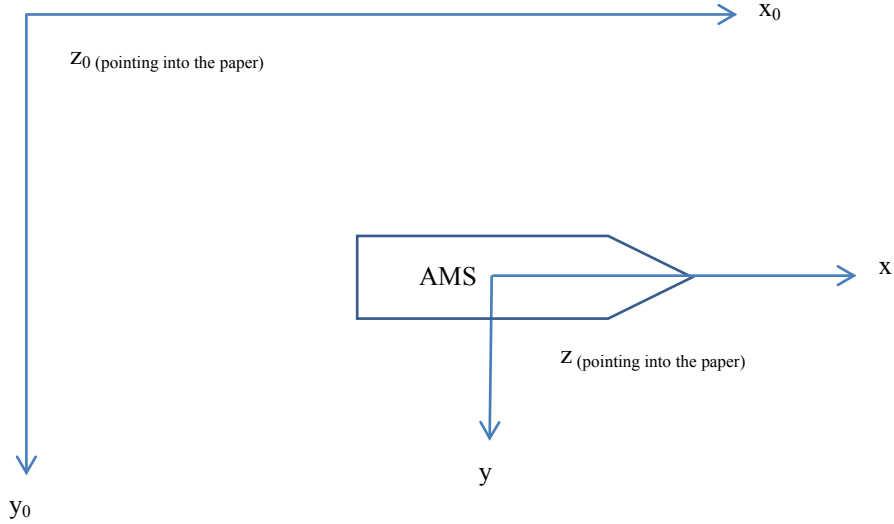


Figure 10. Earth-fixed coordinate system and the ship-fixed coordinate system.

Next, the equations of motion in the horizontal plane (i.e., the xy -plane) that govern the motion of a SAW (or any ship), which are derived in [18], are captured in (1).

$$\begin{aligned} (m - Y_v)\dot{v} - (Y_r - mx_G)\dot{r} &= Y_v v + (Y_r - mU)r + F_{WPB} + Y_\delta \delta \\ (I_z - N_r)\dot{r} - (N_v - mx_G)\dot{v} &= N_v v + (N_r - mx_GU)r + N_{WPB} + N_\delta \delta \end{aligned} \quad (1)$$

In (1),

M : the vessel's mass

v : the velocity in the x-direction (known as the sway velocity)

r : the angular velocity in the clockwise direction (known as the yaw angular velocity)

\dot{v} : the acceleration in the y-direction

\dot{r} : the angular acceleration in the clockwise direction

I_z : the moment of inertia about the z-axis

x_G : the distance along the x-axis from the amidships (AMS) to the ship's center of gravity (CG)

F_{WPB} : the magnitude of the WPB-induced force

N_{WPB} : the magnitude of the torque due to the WPB-induced force

U : the nominal forward speed

$Y_{\dot{v}}$: the change in force in the sway direction per a unit change in the sway acceleration

Y_v : the change in force in the sway direction per a unit change in the sway velocity

$Y_{\dot{r}}$: the change in force in the sway direction per a unit change in the yaw angular acceleration

Y_r : the change in force in the sway direction per a unit change in the yaw angular velocity

Y_{δ} : the change in force in the sway direction per a unit change in the rudder deflection angle

$N_{\dot{v}}$: the change in moment in the yaw rotation per a unit change in the sway acceleration

N_v : the change in moment in the yaw rotation per a unit change in the sway velocity

N_r : the change in moment in the yaw rotation per a unit change in the yaw angular acceleration

N_r : the change in moment in the yaw rotation per a unit change in the yaw angular velocity

N_δ : the change in moment in the yaw rotation per a unit change in the rudder deflection angle

The quantities with the subscripts v , r , \dot{v} , \dot{r} and δ are the hydrodynamics derivatives. The equations of motion (1) are now turned into a system of linear differential equations for the velocity v and the angular velocity r ; that is, \dot{r} and \dot{v} are linear functions of r and v .

$$\begin{aligned} \dot{v} &= \frac{(I_z - N_r)Y_v + (Y_r - mx_G)N_v}{(I_z - N_r)(m - Y_{\dot{v}}) - (Y_{\dot{r}} - mx_G)(N_{\dot{v}} - mx_G)}v + \frac{(I_z - N_r)(Y_r - m) + (Y_{\dot{r}} - mx_G)(N_r - mx_G)}{(I_z - N_r)(m - Y_{\dot{v}}) - (Y_{\dot{r}} - mx_G)(N_{\dot{v}} - mx_G)}r \\ &+ \frac{(I_z - N_r)Y_\delta + (Y_{\dot{r}} - mx_G)N_\delta}{(I_z - N_r)(m - Y_{\dot{v}}) - (Y_{\dot{r}} - mx_G)(N_{\dot{v}} - mx_G)}\delta + \frac{(I_z - N_r)F_{WPB} + (Y_{\dot{r}} - mx_G)N_{WPB}}{(I_z - N_r)(m - Y_{\dot{v}}) - (Y_{\dot{r}} - mx_G)(N_{\dot{v}} - mx_G)} \end{aligned} \quad (2)$$

$$\begin{aligned} \dot{r} &= \frac{(N_{\dot{v}} - mx_G)Y_v + (m - Y_{\dot{v}})N_v}{(I_z - N_r)(m - Y_{\dot{v}}) - (Y_{\dot{r}} - mx_G)(N_{\dot{v}} - mx_G)}v + \frac{(N_{\dot{v}} - mx_G)(Y_r - m) + (m - Y_{\dot{v}})(N_r - mx_G)}{(I_z - N_r)(m - Y_{\dot{v}}) - (Y_{\dot{r}} - mx_G)(N_{\dot{v}} - mx_G)}r \\ &+ \frac{(N_{\dot{v}} - mx_G)Y_\delta + (m - Y_{\dot{v}})N_\delta}{(I_z - N_r)(m - Y_{\dot{v}}) - (Y_{\dot{r}} - mx_G)(N_{\dot{v}} - mx_G)}\delta + \frac{(N_{\dot{v}} - mx_G)F_{WPB} + (m - Y_{\dot{v}})N_{WPB}}{(I_z - N_r)(m - Y_{\dot{v}}) - (Y_{\dot{r}} - mx_G)(N_{\dot{v}} - mx_G)} \end{aligned}$$

Note that, in this work, no environmental disturbances, such as wind, currents, or waves, are considered, and the rudder deflection angle is zero degree. Using the water density ρ , the ship length L , and the nominal forward speed U , the variables can be nondimensionalized as shown in (3). The dimensionless form of the equations of motion in the primed variables turns out to be identical to that of (1) and (2) with $U'=1$. Unless stated otherwise, this work assumes the dimensionless form of the equations of motion, , and, for convenience, the primes are dropped.

$$\begin{aligned}
v' &= \frac{v}{U}, r' = \frac{rL}{U}, \dot{v}' = \frac{\dot{v}L}{U^2}, \dot{r}' = \frac{\dot{r}L^2}{U^2}, \\
t' &= \frac{tU}{L}, m' = \frac{m}{\frac{1}{2}\rho L^3}, I_z' = \frac{I_z}{\frac{1}{2}\rho L^5}, x'_G = \frac{x_G}{L}, \\
Y_{\dot{v}}' &= \frac{Y_{\dot{v}}}{\frac{1}{2}\rho L^3}, Y_{\dot{r}}' = \frac{Y_{\dot{r}}}{\frac{1}{2}\rho L^4}, N_{\dot{v}}' = \frac{N_{\dot{v}}}{\frac{1}{2}\rho L^4}, N_{\dot{r}}' = \frac{N_{\dot{r}}}{\frac{1}{2}\rho L^5}, \\
Y_v' &= \frac{Y_v}{\frac{1}{2}\rho L^2 U}, Y_r' = \frac{Y_r}{\frac{1}{2}\rho L^3 U}, N_v' = \frac{N_v}{\frac{1}{2}\rho L^3 U}, N_r' = \frac{N_r}{\frac{1}{2}\rho L^4 U}, \\
Y_{\delta}' &= \frac{Y_{\delta}}{\frac{1}{2}\rho L^2 U^2}, N_{\delta}' = \frac{N_{\delta}}{\frac{1}{2}\rho L^3 U^2},
\end{aligned} \tag{3}$$

The evaluation of the hydrodynamics derivatives, which are dimensionless, is discussed in Section A of Chapter VI.

2. Parameters

The equations of motion in (1) or the equations in (2) contain two types of parameters: fixed and variable parameters. The variable parameters are the magnitude of F_{WPB} and the magnitude of the torque N_{WPB} , whose value depends on the location of application of F_{WPB} and the magnitude of F_{WPB} (the angle of application being 90°). Different values of the magnitude of F_{WPB} are based on a nominal value, whose estimation using ship hydrostatics is elaborated in Section B of Chapter IV. While not a parameter inherent in the equations of motion, the duration of application of F_{WPB} is also considered in the study of the response of the SAW to the application of F_{WPB} over a small, finite duration of time. The parametric nature of the study thus reflects the variation of the magnitude of F_{WPB} , the location of application of F_{WPB} , and the duration of application of F_{WPB} .

The fixed parameters are the hydrodynamics derivatives, the SAW mass, m , the moment of inertia about the z-axis, I_z , and the distance along the x-axis from the amidships (AMS) to the ship's center of gravity (CG), x_G . The latter three parameters are related to the SAW characteristics. The hydrodynamics derivatives are computed using

the maneuvering prediction program (MPP1.3) [19], which uses as input the vessel and operating environment characteristics described in Chapter II. Appendix A contains the details of MPP1.3.

3. Ship Kinematics

Given an initial condition of \mathbf{randv} , integration of the system in (2) yields r, v, \dot{r} and \dot{v} as functions of time t . The yaw angle, ψ , is measured counterclockwise with respect to the x_0 -axis. It can be obtained by integrating $\dot{\psi}$, the yaw velocity (in the clockwise direction), with respect to time t . In particular, over a sufficiently small time interval $[t, t + \Delta t]$, ψ is given by

$$\psi(t + \Delta t) = \psi(t) + \dot{\psi}(t)\Delta t \quad (4)$$

or, since $\dot{\psi}$ is equal to r ,

$$\psi(t + \Delta t) = \psi(t) + r(t)\Delta t \quad (5)$$

Finally, the kinematical variables in the earth-fixed frame, x_o, y_o, \dot{x}_o and \dot{y}_o , are obtained according to

$$\begin{aligned} \dot{x}_o(t) &= u(t) \cos \psi(t) - v(t) \sin \psi(t) \\ \dot{y}_o(t) &= u(t) \sin \psi(t) + v(t) \cos \psi(t) \\ x_o(t + \Delta t) &= x_o(t) + \dot{x}_o(t)\Delta t \\ y_o(t + \Delta t) &= y_o(t) + \dot{y}_o(t)\Delta t \end{aligned} \quad (6)$$

where u is the velocity in the y -direction (known as the surge velocity).

B. NOMINAL WPB-INDUCED FORCE CALCULATION

A simplified representation of a stationary ship in water is a rectangular block immersed in undisturbed water, assumed to be incompressible, non-viscous, and with no surface tension. The ship is in an equilibrium state when the drafts at forward, aft, port and starboard are equal.

The free-body diagram in Figure 11 shows the hydrostatic forces exerted on the ship in its equilibrium state. The weight of the ship is denoted by W . The buoyancy force

$(\vec{F}_{\text{Buoyancy}})$ is the upward vertical force exerted by the water; its magnitude equals to the weight of the fluid displaced. The horizontal forces (\vec{F}_{S3} and \vec{F}_{S4}) exerted by the water are of equal magnitudes but point in the opposite direction. The net force in the horizontal direction is thus zero. The magnitudes of these forces are calculated according to (7).

$$\begin{aligned} F_{S3} = F_{S4} &= L \int_0^T \rho g z dz = \frac{1}{2} L \rho g T^2 \\ F_{\text{Buoyancy}} &= \rho g L B T \end{aligned} \quad (7)$$

where L is the length of the ship, B the breath of the ship, T the draft of the ship, z the distance from the water surface to the center of pressure (or the depth of pressure), ρ the density of the seawater, and g the gravitational acceleration.

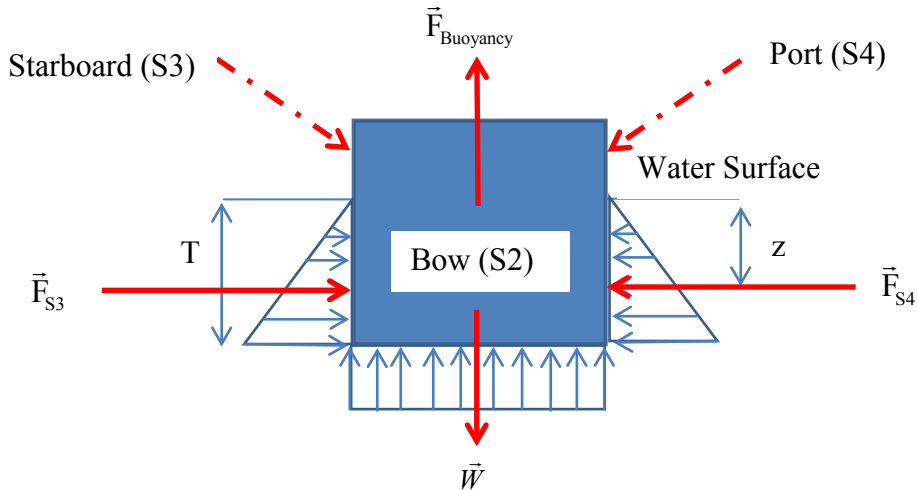


Figure 11. Hydrostatic force on a ship body at equilibrium

Figure 12 depicts the changes in the hydrostatic forces when a WPB is applied to the ship. As the WPB is applied, the forward draft (T) at the starboard would be increased by αT , for $0 < \alpha < 1$, thereby creating an additional force, \vec{F}_y , in the negative y -direction. The resultant horizontal force, \vec{F}_{S3}^1 , which is the sum of \vec{F}_{S3} and \vec{F}_y , is now

greater than \vec{F}_{S4} , causing the ship to roll by an angle Φ and resulting in $\vec{F}_{Buoyancy}^1$, which deviates from the z-axis by the same angle, Φ .

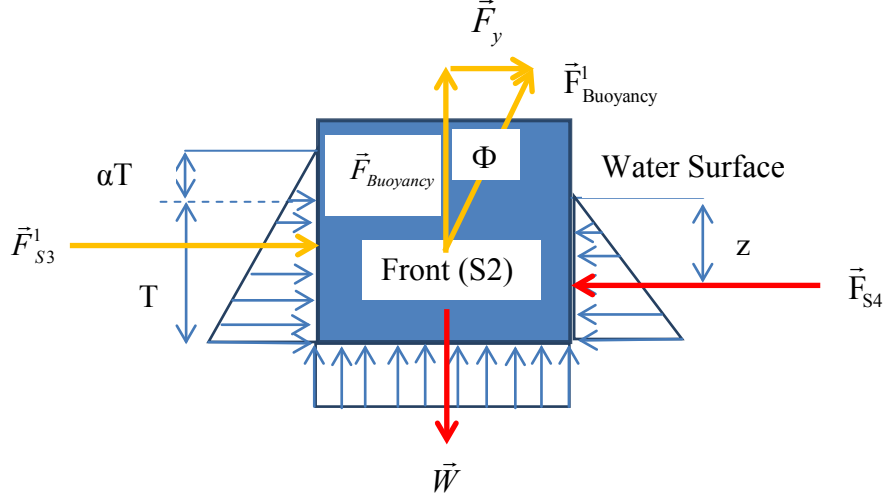


Figure 12. Changes in the hydrostatic forces

With the application of the WPB,

$$\begin{aligned}
 F_{Buoyancy}^1 &= \frac{1}{2} \rho g L B [T + T(1 + \alpha)] \\
 \Phi &= \tan^{-1} \left(\frac{\alpha T}{B} \right) \\
 F_y &= F_{Buoyancy}^1 \sin \Phi
 \end{aligned} \tag{8}$$

The WPB is assumed to be applied at some location in the forward area of the ship. The footprint of the WPB on the SAW (i.e., the length of the WPB that actually interacts with the SAW) covers a fraction of the hull of the SAW, denoted by β , which takes values in $(0, 1)$. The magnitude of the resultant hydrostatic force, or the WPB-induced force, \vec{F}_{WPB} , exerted on the hull is then given by

$$F_{WPB} = F_y \beta = F_{Buoyancy}^1 \sin \Phi \beta = \frac{1}{2} \rho g L B [T + T(1 + \alpha)] \sin \Phi \beta \tag{9}$$

This \vec{F}_{WPB} is the nominal WPB-induced force to be used in the generation of variants of the WPB-induced forces considered in the parametric study.

The location of application of the WPB-induced force, assumed to be in the fore section of the hull, is at a distance of γL from the bow, where $0 < \gamma < \frac{1}{2}$, and a distance l (the moment arm of \vec{F}_{WPB}) from the amidships (AMS). As the geometry in Figure 13 shows, $l = \left(\frac{1}{2} - \gamma\right)L$. The magnitude N_{WPB} of the moment resulting from the application of the WPB-induced force, \vec{F}_{WPB} , perpendicular to the hull is then given by

$$N_{WPB} = lF_{WPB} = \left(\frac{1}{2} - \gamma\right)LF_{WPB} \quad (10)$$

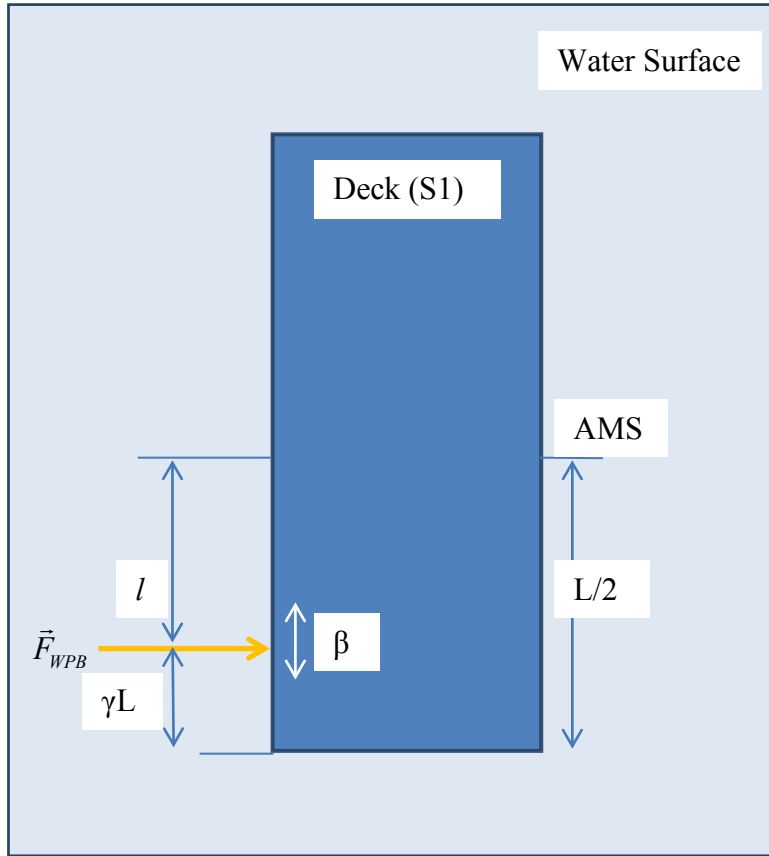


Figure 13. Plan view of the SAW and location of the applied F_{WPB}

C. SOLUTION IMPLEMENTATION

1. Calculation of Parameters

Tables 3 and 4 summarize the input parameters. Two counter-SAW operational assumptions are made in the determination of the magnitude of the nominal WPB-induced force.

- 1) The factor α (introduced in Chapter IV) by which the SAW draft is increased by the application of a WPB is set to be 0.3.
- 2) The footprint β is set to be 0.3.

With the roll angle Φ obtained from (7) and the values of ρ , g , L , B , and T given in Table 2 in Chapter II, the calculation of the magnitude of the nominal WPB-induced force, F_{WPB} , using (8), results in $F_{WPB} = 82.7 \times 10^6$ N.

The location of \vec{F}_{WPB} application varies between 0.1L and 0.25L from the bow tip.

The duration of \vec{F}_{WPB} application varies between 1 to 2.5 seconds.

The values of the hydrodynamics derivatives in Table 4 are generated by the maneuvering prediction program (MPP1.3) mentioned in Section A of Chapter IV. The values of the derivatives are unitless.

Table 3. Values for F_{WPB} , location and duration of F_{WPB} application

S/No.	INPUT PARAMETERS	NOTATION	VALUE
1.	Magnitude of WPB-induced force (N)	F_{WPB}	82.7×10^6 to 206.8×10^6
2.	Location of F_{WPB} application (m)	l	0.1L to 0.25L
3.	Duration of F_{WPB} application (s)		1 to 2.5
4.	Dimensionless mass	m	0.017620
5.	Dimensionless moment of inertia	I_z	0.001101

Table 4. Values of hydrodynamic derivatives

S/No.	INPUT PARAMETERS	NOTATION	VALUE
1.	The change in force in the sway direction per a unit change in the sway velocity	Y_v	-0.025566
2.	The change in force in the sway direction per a unit change in the sway acceleration	$Y_{\dot{v}}$	-0.016110
3.	The change in force in the sway direction per a unit change in the yaw angular velocity	Y_r	-0.008402
4.	The change in force in the sway direction per a unit change in the yaw angular acceleration	$Y_{\ddot{r}}$	-0.001046
5.	The change in moment in the yaw rotation per a unit change in the sway velocity	N_v	0.005079
6.	The change in moment in the yaw rotation per a unit change in the sway acceleration	$N_{\dot{v}}$	-0.001200
7.	The change in moment in the yaw rotation per a unit change in the yaw angular velocity	N_r	-0.003691
8.	The change in moment in the yaw rotation per a unit change in the yaw angular acceleration	$N_{\ddot{r}}$	-0.000870
9.	The change in force in the sway direction per a unit change in the rudder deflection angle	Y_{δ}	0.003275
10.	The change in moment in the yaw rotation per a unit change in the rudder deflection angle	N_{δ}	-0.001605

2. MATLAB Implementation

The equations of motion in (2), (5) and (6) are coded using MATLAB, and the resulting code is run with the values of the parameters in Tables 3 and 4 to generate the results for the parametric analysis. Appendix B contains the MATLAB code.

a. MATLAB Inputs

(1) Code Execution Data. The code is executed for five seconds with a time step Δt of 0.001 seconds.

(2) Hydrodynamic Derivatives. Table 4 contains the values of the hydrodynamics derivatives obtained with MPP1.3, as discussed in Section A of Chapter IV. The vessel and operating environment characteristics described in Chapter II are inputs to MPP1.3.

(3) Nominal F_{WPB} . As shown in Table 3, the nominal magnitude of the WPB-induced force F_{WPB} is 82.7×10^6 N.

(4) Initial Conditions. The initial conditions refer to the kinematical variables at the time immediately prior to the application of F_{WPB} .

(5) Parametric Study Data. Four different magnitudes of the WPB-induced force, F_{WPB} , are considered: 82.7×10^6 N, corresponding to the nominal value, 82.7×10^6 N (Force #1), 124.1×10^6 N (Force #2), 165.4×10^6 N (Force #3), and 206.8×10^6 N (Force #4). Each of these forces can be applied to four different locations along the hull; they correspond to four different values of γ : 0.1, 0.15, 0.2, and 0.25. For each of these forces and each location of its application, four different durations of the WPB-induced force application are considered: 1, 1.5, 2, and 2.5 seconds. The application of these forces always starts at 1.0 second.

b. MATLAB Outputs

For each combination of the three parameters — the magnitude of the WPB-induced force, the location of its application along the hull of the SAW, and the duration of its application of the WPB-induced force, the following outputs are obtained and displayed graphically.

(1) Angular Deviation of SAW Path. The angle θ between the SAW's intended destructive course and its deflected path resulting from the application of WPB is computed as a function of time. The deflected path is along the bearing direction when

the application of F_{WPB} stops. This result is used in the assessment of the counter-SAW mission success.

(2) SAW Motion in Ship-fixed Coordinate System. The SAW acceleration \dot{v} in the sway direction, the angular acceleration \dot{r} in the clockwise direction, the velocity v in the y-direction are obtained as functions of time. These outputs are to illuminate the SAW motion in both coordinate systems.

THIS PAGE INTENTIONALLY LEFT BLANK

V. PARAMETRIC STUDY RESULTS AND DISCUSSION

As previously discussed, the three parameters that are varied in this parametric study are: the magnitude of the WPB-induced force, the location of its application along the hull of the SAW, and the duration of the application of the WPB-induced force. The objective of the parametric study is to determine a combination or combinations of these three parameters that satisfy the counter-SAW mission success requirement.

As discussed in Chapter IV, $\dot{r}, r(t), \dot{v}, v(t)$ and θ stand for the angular acceleration, the angular velocity, the acceleration in the sway direction, the velocity in the y-direction, and the deflection angle, respectively. The parametric study results of $\{\dot{r}, r(t), \dot{v}, v(t)\}$ and $\{\theta\}$ are obtained for the following three combinations of the parameters.

- 1) Variable F_{WPB} , a fixed location of \vec{F}_{WPB} application, and a fixed duration of \vec{F}_{WPB} application.
- 2) A fixed F_{WPB} , variable locations of \vec{F}_{WPB} application, and a fixed duration of \vec{F}_{WPB} application.
- 3) A fixed F_{WPB} , a fixed location of \vec{F}_{WPB} application, and variable durations of \vec{F}_{WPB} application.

A. COMBINATION 1—VARIABLE MAGNITUDE OF \vec{F}_{WPB}

Figures 14 and 15 show the temporal evolution of \dot{v} and \dot{r} , respectively, for the four indicated forces, the location and duration of \vec{F}_{WPB} application remaining fixed at $\gamma = 0.15$ and one second, respectively. The sway acceleration, \dot{v} , and the angular acceleration, \dot{r} , reach their peak values when each of these forces is applied and, because the resistance of the hydrodynamic force overcomes F_{WPB} , they rapidly decrease until the \vec{F}_{WPB} application ends, at which time they peak again but in the opposite direction. They then decrease rapidly to zero due to the damping effects. The damping effects refer to the

effects of the resistance of the hydrodynamic force. Furthermore, the largest sway acceleration and the largest angular acceleration correspond to the largest magnitude of \vec{F}_{WPB} (i.e., Force #4).

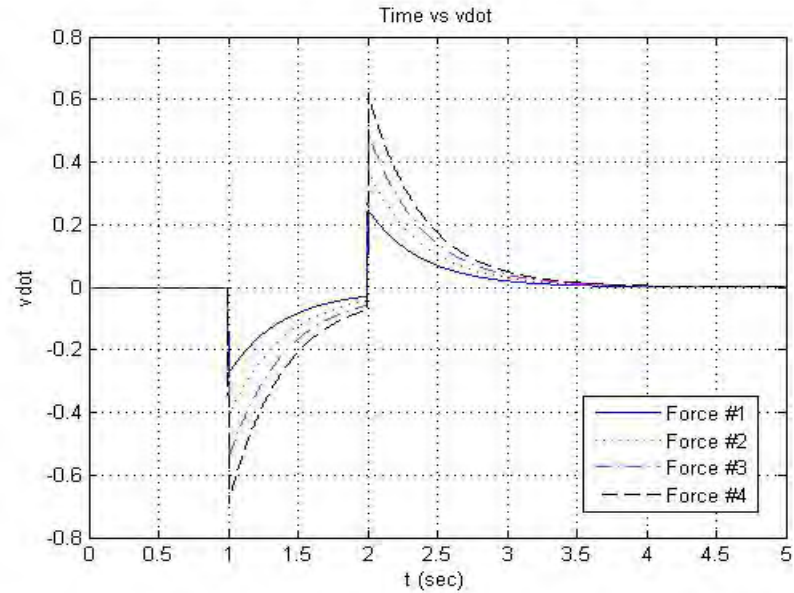


Figure 14. Time vs \dot{v}

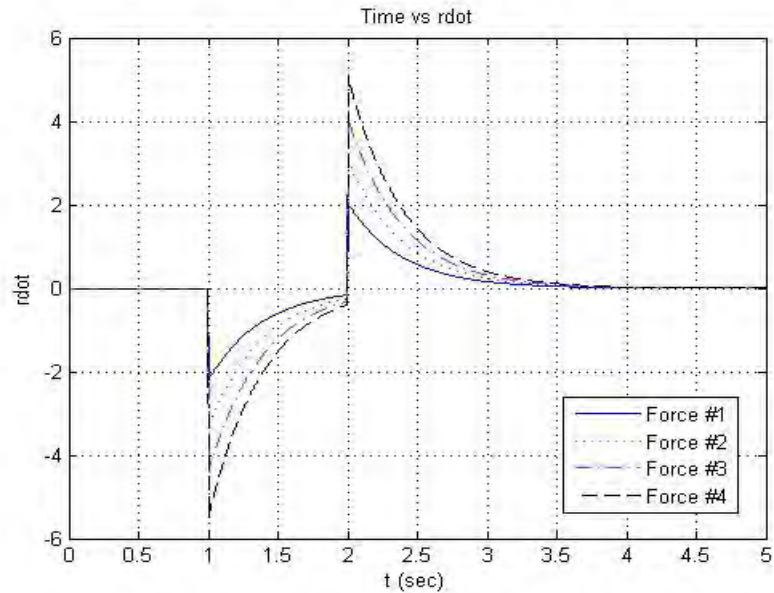


Figure 15. Time vs \dot{r}

Figures 16 and 17 show the temporal evolution of v and r , respectively, for the four indicated forces, the location and duration of \vec{F}_{WPB} application remaining fixed at $\gamma = 0.15$ and one second, respectively. During the \vec{F}_{WPB} application, the velocity, v , and the angular velocity, r , rapidly reach their peak values and, when the \vec{F}_{WPB} application ends, they decrease rapidly to zero because of the damping effects. Furthermore, the largest velocity and angular velocity correspond to the largest magnitude of \vec{F}_{WPB} (i.e., Force #4).

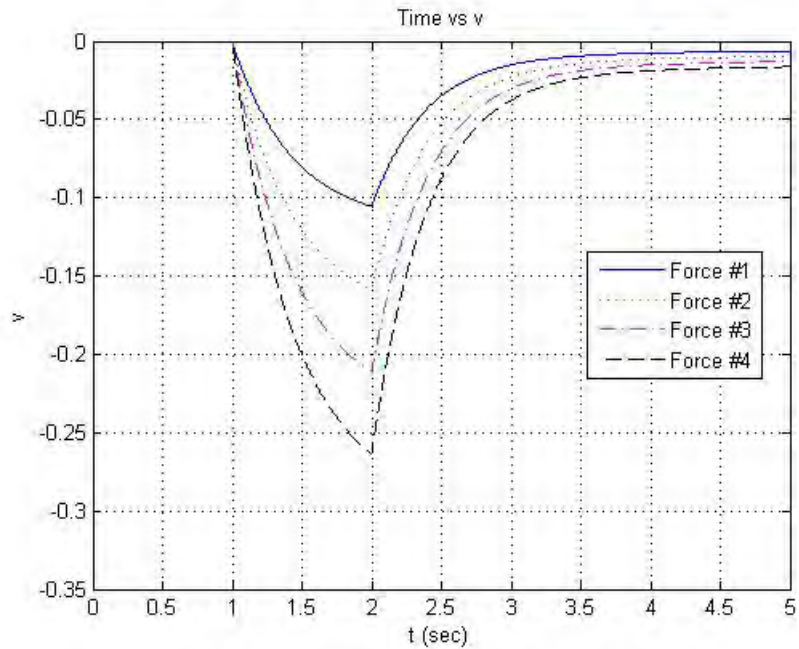


Figure 16. Time vs v

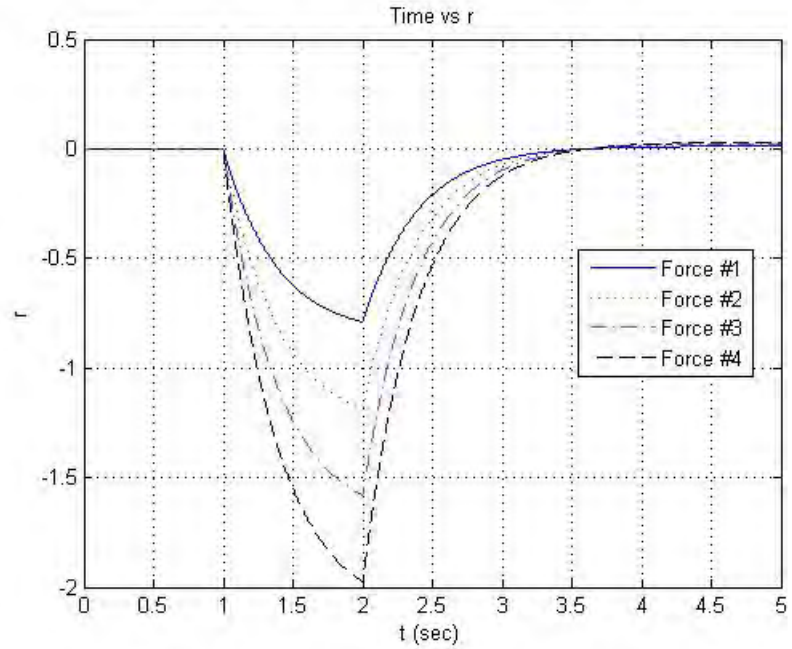


Figure 17. Time vs r

Figure 18 shows the temporal evolution of the deflection angle θ for the four indicated forces, the location and duration of F_{WPB} application remaining fixed at $\gamma = 0.15$ and one second, respectively. It takes 2.3 seconds to achieve the required deflection angle of 30° with the largest magnitude of the WPB-induced force and about 4.5 seconds with its smallest magnitude.

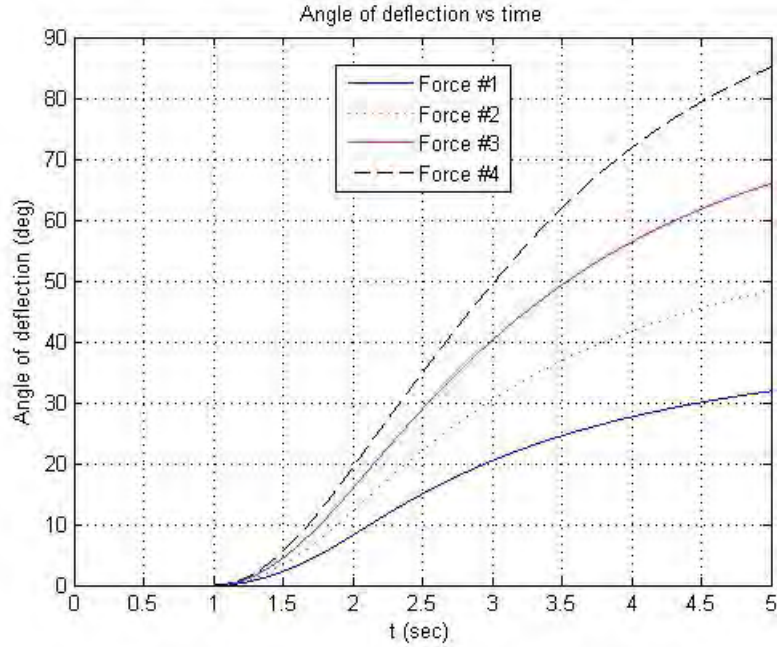


Figure 18. Angle of deflection vs time

This set of results thus indicates that the high magnitude of the WPB-induced force is more effective in diverting the destructive course than does to the low magnitude. The required deflection angle of 30° is achieved more quickly with the high magnitude than with the low magnitude of the WPB-induced force.

B. COMBINATION 2—VARIABLE LOCATION OF \vec{F}_{WPB} APPLICATION

Figures 19 shows the temporal evolution of the sway acceleration, \dot{v} , for the four indicated locations of \vec{F}_{WPB} application, the magnitude of the applied \vec{F}_{WPB} and the duration of \vec{F}_{WPB} application remaining fixed at 82.7×10^6 N and one second, respectively. The temporal behavior of \dot{v} is identical to that of \dot{v} in Figure 14, irrespective of the location of \vec{F}_{WPB} application, in the sense that \dot{v} reaches its peak value when \vec{F}_{WPB} is applied and, because the resistance of the hydrodynamic force overcomes the F_{WPB} , it rapidly decreases until the \vec{F}_{WPB} application ends, at which time it peaks again but in the opposite direction. It then decreases rapidly to zero due to the damping effects.

As the location of \vec{F}_{WPB} application recedes from the bow (i.e., γ increases), the applied moment N_{WPB} decreases. The largest moment results in the smallest sway acceleration as the translation effect is at the minimum. However, as shown in Figure 20, the largest angular acceleration, $\dot{\gamma}$, corresponds to the largest moment as it produces the largest rotation effect.

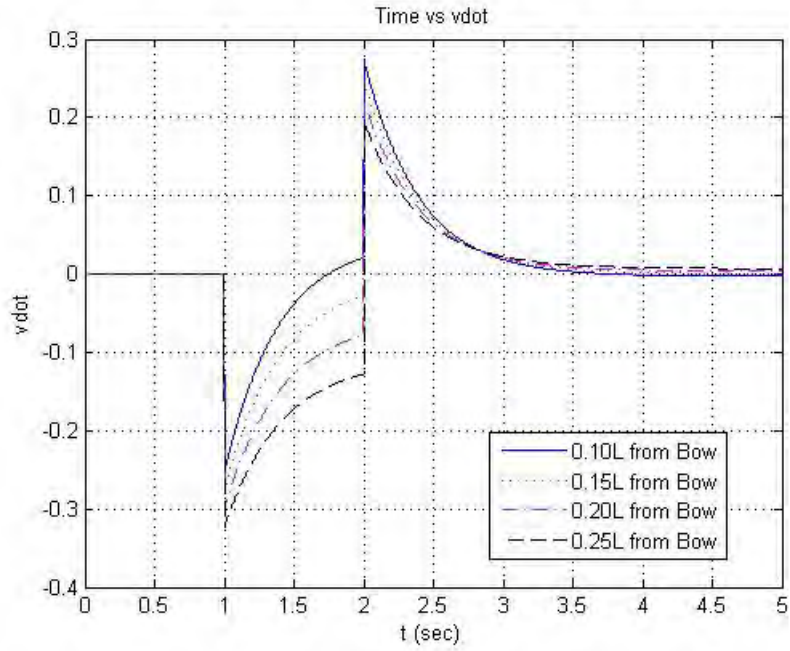


Figure 19. Time vs $\dot{\gamma}$

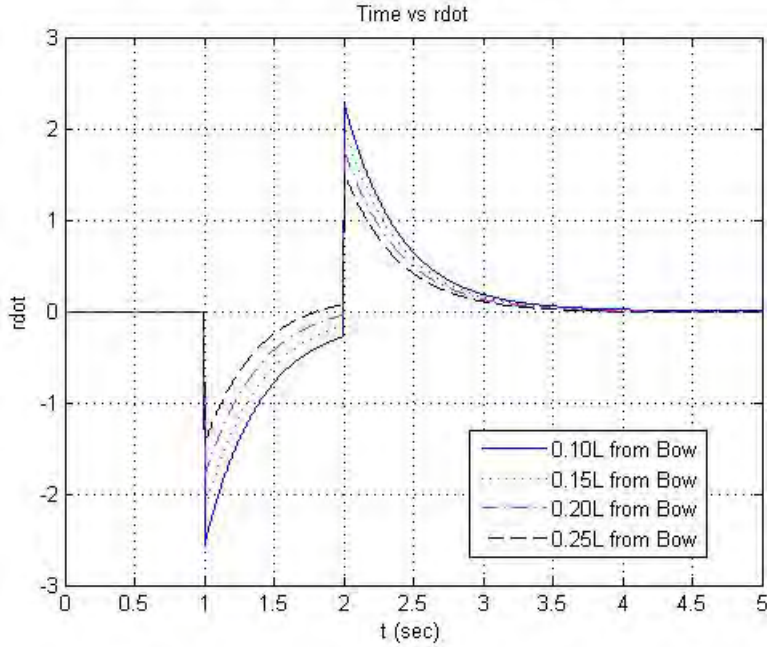


Figure 20. Time vs \dot{r}

Figures 21 and 22 show the temporal evolution of v and r , respectively, for the four indicated locations of \vec{F}_{WPB} application, the magnitude of the applied \vec{F}_{WPB} and the duration of \vec{F}_{WPB} application remaining fixed at 82.7×10^6 N and one second, respectively. During the \vec{F}_{WPB} application, the velocity, v , and the angular velocity, r , rapidly reach their peak values and, when the \vec{F}_{WPB} application ends (i.e., the application of the moment ends), they decrease rapidly to some values because of the damping effects. As the location of \vec{F}_{WPB} application recedes from the bow (i.e., γ increases), the applied moment N_{WPB} decreases. The largest moment results in the smallest velocity as the translation effect is at the minimum. However, as shown in Figure 22, the largest the angular velocity, r , corresponds to the largest moment as it produces the largest rotational effect. The smaller the moment is, the greater the SAW restoring moment is; the resulting effect is an increase of the angular velocity in the positive region.

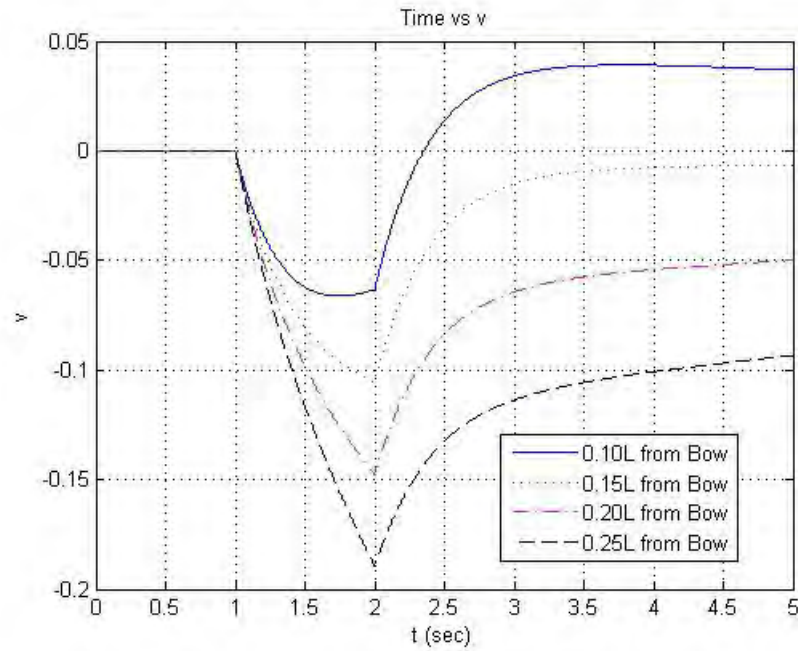


Figure 21. Time vs v

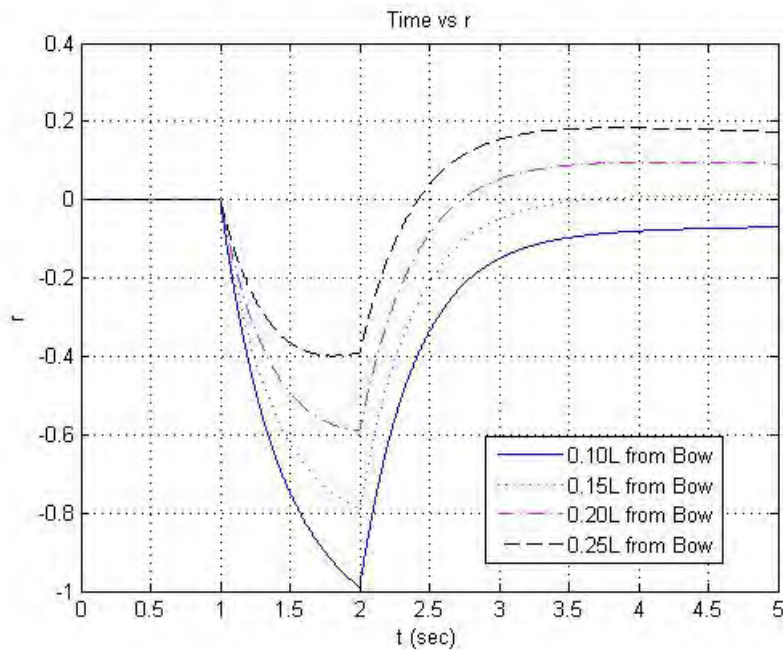


Figure 22. Time vs r

Figure 23 shows the temporal evolution of the deflection angle θ for the four indicated locations of \vec{F}_{WPB} application, the magnitude of the applied \vec{F}_{WPB} and the duration of \vec{F}_{WPB} application remaining fixed at 82.7×10^6 N and one second, respectively. The location of \vec{F}_{WPB} application closest to the bow ($\gamma = 0.1$), hence the largest moment, allows the required deflection angle of 30° to be achieved in 3.6 seconds, the smallest amount of time as compared to those corresponding to the other locations of \vec{F}_{WPB} application.

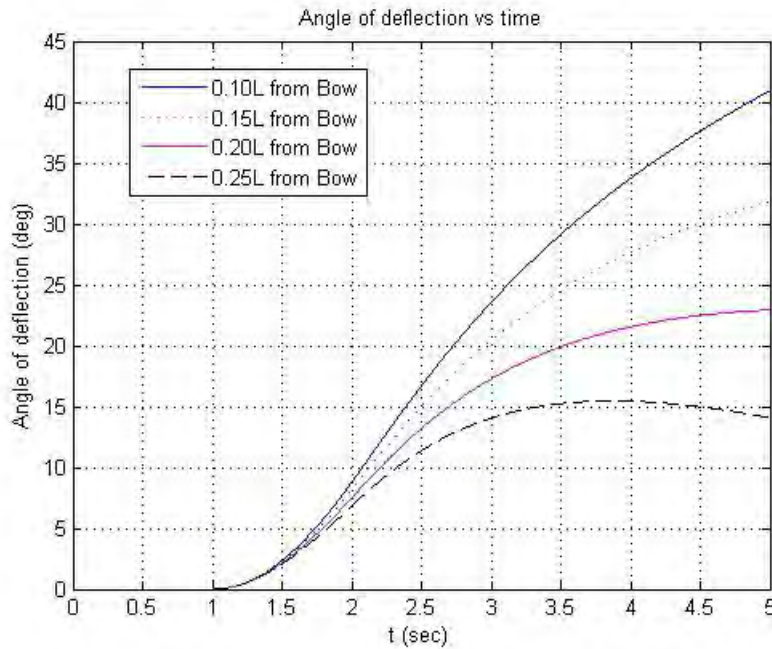


Figure 23. Angle of deflection vs time

This set of results thus indicates that the greater moments are more effective in diverting the destructive course than do the greater moments. The required deflection angle of 30° is achieved more quickly with the moment arms corresponding to $\gamma = 0.1$ and 0.15 than with the other moment arms.

C. COMBINATION 3—VARIABLE DURATION OF \vec{F}_{WPB} APPLICATION

Figures 24 and 25 show the temporal evolution of \dot{v} and \dot{r} , respectively, for the four indicated durations of \vec{F}_{WPB} application, the magnitude of \vec{F}_{WPB} and the location of

\vec{F}_{WPB} application remaining fixed at 82.7×10^6 N and $\gamma = 0.15$, respectively. The sway acceleration, \dot{v} , and the angular acceleration, \dot{r} , reach their peak values when each of these forces is applied and, because the resistance of the hydrodynamic force overcomes \vec{F}_{WPB} , they rapidly decrease until the \vec{F}_{WPB} application ends, at which time they peak again but in the opposite direction. They then decrease rapidly to zero due to the damping effects. Furthermore, the times at which they peak in the opposite direction naturally reflect the durations of \vec{F}_{WPB} application. The temporal evolution profiles of \dot{v} and \dot{r} are identical, irrespective of the durations of \vec{F}_{WPB} application, because the magnitude of \vec{F}_{WPB} and the location of \vec{F}_{WPB} application are fixed.

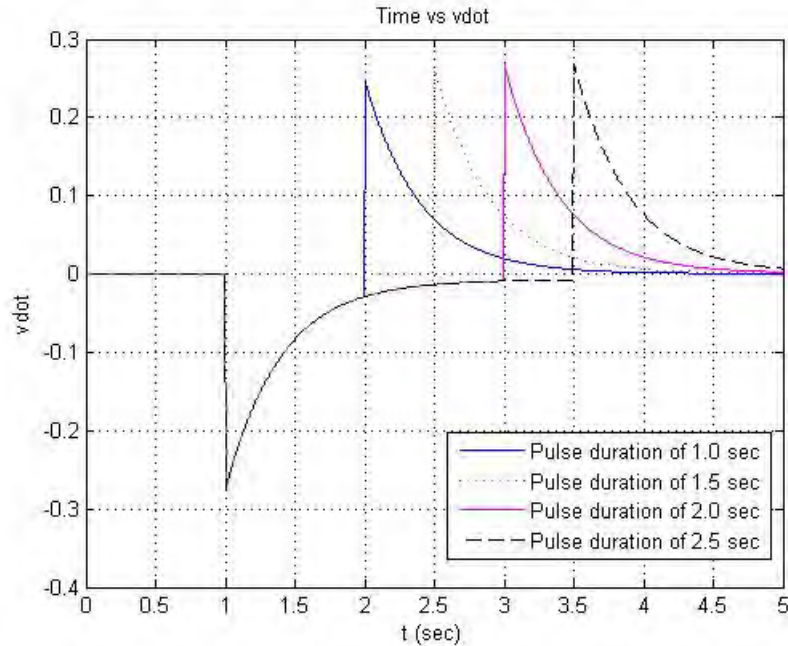


Figure 24. Time vs \dot{v}

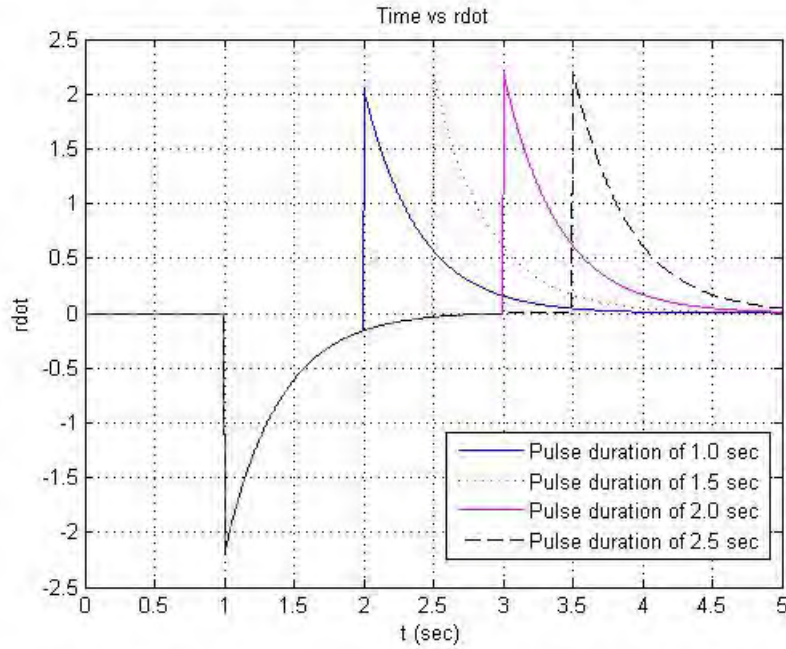


Figure 25. Time vs \dot{r}

Figures 26 and 27 show the temporal evolution of v and r , respectively, for the four indicated durations of \vec{F}_{WPB} application, the magnitude of \vec{F}_{WPB} and the location of \vec{F}_{WPB} application remaining fixed at 82.7×10^6 N and $\gamma = 0.15$, respectively. During the F_{WPB} application, the velocity, v , and the angular velocity, r , rapidly reach their peak values and, when the F_{WPB} application ends, they decrease rapidly to zero because of the damping effects. Furthermore, the larger the duration of \vec{F}_{WPB} application, the longer the duration of the rapid increase of v and r during the acceleration phase, and the smaller the time it takes v and r to rapidly decrease during the deceleration phase.

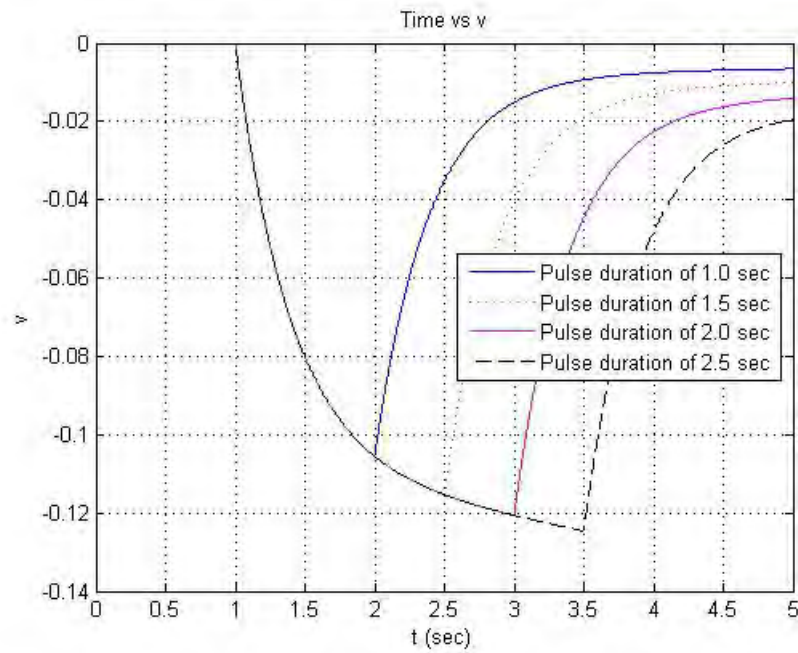


Figure 26. Time vs v

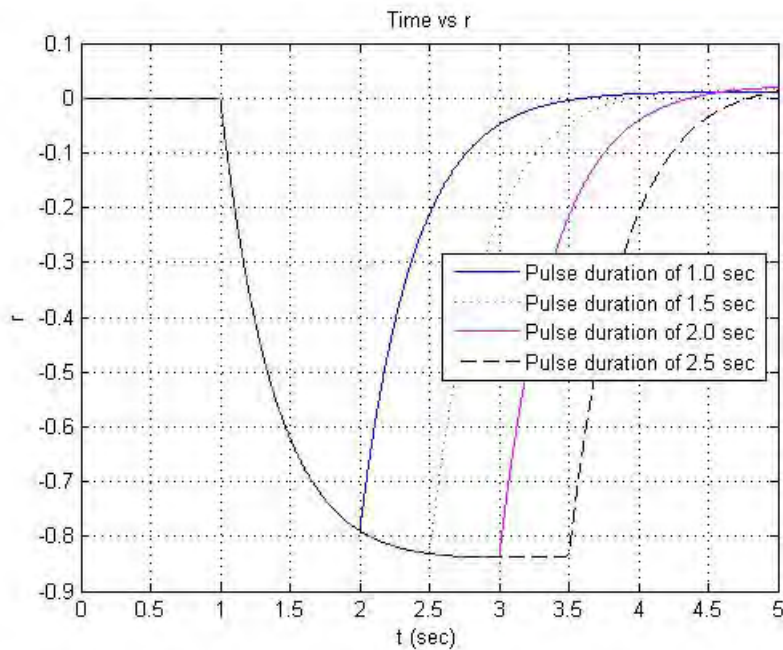


Figure 27. Time vs r

Figure 28 shows the time that is required to achieve the deflection angle of 30° , for the four indicated durations of \vec{F}_{WPB} application, the magnitude of \vec{F}_{WPB} and the location of \vec{F}_{WPB} application remaining fixed at $82.7 \times 10^6 \text{ N}$ and $\gamma = 0.15$, respectively. For the 2.5-second duration of \vec{F}_{WPB} application, it takes about 3.2 seconds to reach the required deflection angle. An amount of 4.5 seconds is needed to reach required deflection angle for the 1.0-second duration of \vec{F}_{WPB} application.

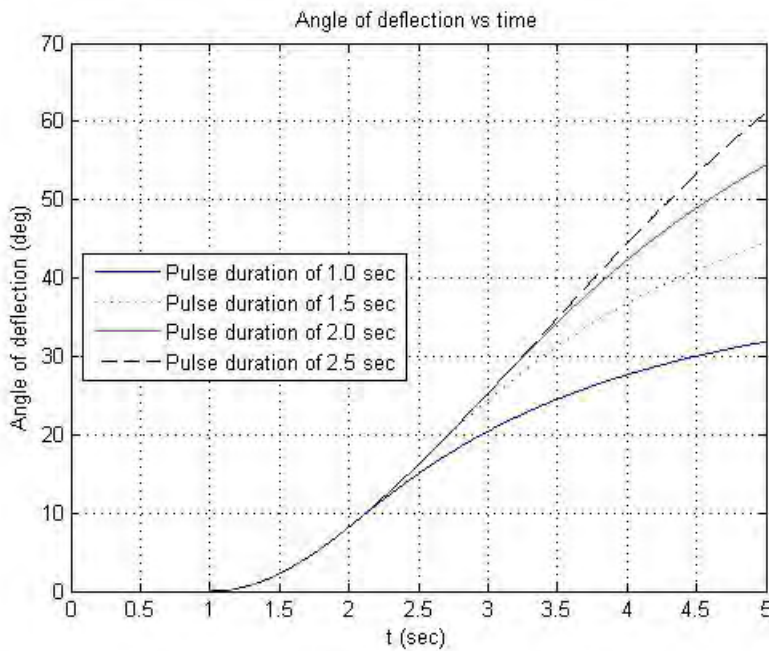


Figure 28. Angle of deflection vs time

This set of results thus indicates that the long durations of \vec{F}_{WPB} application are more effective in diverting the SAW destructive course than do the short durations. The longer durations result in reaching the required deflection angle faster.

The obtained results presented in this chapter are used in the preliminary assessment of the feasibility of using a WPS to counter a SAW, which is discussed in the next chapter.

THIS PAGE INTENTIONALLY LEFT BLANK

VI. PRELIMINARY ASSESSMENT

An assessment of the feasibility of using a WPB to counter a SAW amounts to answering to the questions posed in the problem stated in Chapter I: Is it feasible to apply WPB-induced forces to the hull of the SAW to alter its destructive course? If feasible, what are the magnitudes of the WPB-induced forces and for how long do they need to be maintained? Where on the hull of the SAW should they be applied? Put differently, which combinations of the three parameters — the magnitude of the WPB-induced force, the location of its application along the hull of the SAW, and the duration of its application of the WPB-induced force — satisfy the counter-SAW mission requirement of steering the SAW 30° off its destructive course established in Chapter II. This chapter provides this assessment.

A. SUMMARY OF PARAMETRIC STUDY RESULTS

Table 5. Summary of parametric study results

WPB-Induced Force, F_{WPB} (N)	Location of F_{WPB} Application, γ	Duration of F_{WPB} Application (s)	Time to Deflection Angle of 30° (s)
Variable	Fixed	Fixed	
82.7 x 10 ⁶	0.15	1	4.5
124.1 x 10 ⁶			3
165.4 x 10 ⁶			2.5
206.8 x 10 ⁶			2.3
Fixed	Variable	Fixed	
82.7 x 10 ⁶	0.1	1	3.5
	0.15		4.5
	0.2		∞
	0.25		∞
Fixed	Fixed	Variable	
82.7 x 10 ⁶	0.15	1	4.5
		1.5	3.4
		2	3.2
		2.5	3.2

The parametric study results captured in Table 5 indicate that large magnitudes of \vec{F}_{WPB} result in satisfying the counter-SAW mission success requirement of 30° angle of deflection in short times. A \vec{F}_{WPB} of 82.7 x 10⁶ N magnitude applied for one second at a

location between 0.1 and 0.5 the length (L) of the SAW from its bow takes 4.5 seconds to achieve the deflection angle of 30°. Since the SAW moving at 12.86 m/s would reach its intended target on Jurong Island in at least five minutes from a standoff distance of four kilometers from the target, this combination of the magnitude of the WPB-induced force, the location of its application along the hull of the SAW, and the duration of its application of the WPB-induced force should sufficiently satisfy the counter-SAW mission success requirement.

This combination serves as the preliminary requirements that a WPB impart a force of 82.7×10^6 N magnitude that is exerted for one second at a location along the SAW hull somewhere between 0.1L and 0.15L from the bow.

THIS PAGE INTENTIONALLY LEFT BLANK

VII. CONCLUSION AND RECOMMENDATIONS

This chapter recapitulates the problem, provides a summary of the research findings, and recommendations for future work.

A. CONCLUSION

The specific SAW problem addressed in this thesis involves an oil tanker, Ocean Jewel, commandeered by terrorists to ram a petrochemical processing plant located at the southernmost end of Jurong Island in the Singapore Strait. If sunk or destroyed as a result of a counter measure, the SAW's collateral damage would severely disrupt the traffic flow in the shipping lane. To prevent such a disruptive catastrophe, non-destructive measures must be implemented to cause the oil tanker to deviate from its destructive path toward the target. One such a measure involves a strategic application of WPB-induced forces to the SAW. A WPB is the free water surface that is being pushed up by the bubbles created by, for example, underwater explosions. This thesis examines the feasibility of using a strategically created WPB to alter the destructive course of the SAW.

The feasibility is assessed from two aspects: (1) The effectiveness of a combination of the magnitude of the WPB-induced force, the location of its application along the hull of the SAW, and the duration of its application in diverting the SAW from its path toward its target and (2) the feasibility of generating a WPB that can be used as specified by the combination.

The research captured in this thesis deals mainly with the first feasibility aspect. The findings in this research indicate that it is feasible to use a WPB to counter the SAW. Specifically, at a standoff distance of four kilometers from its targeted plant on Jurong Island, the SAW can be diverted by 30° from its path toward the target by a WPB-induced force of 82.7×10^6 N magnitude exerted for one second at a location along the SAW hull somewhere between 0.1L and 0.15L from the bow. The WPB length covers a fraction of 0.3 of the hull of the SAW and the force increases the saw draft by a factor of 0.3.

The feasibility of generating a WPB that can produce a force of the required magnitude that can be sustained for the required duration is currently investigated by National University of Singapore.

B. RECOMMENDATIONS FOR FUTURE WORK

In Section C of Chapter IV, the factor, α , by which the SAW draft is increased and the footprint of the WPB, β , are both assumed to be 0.3. A future effort is recommended to determine other values for these quantities for which the use of a WPB to counter the SAW is feasible. Furthermore, it is recommended that the on-going NUS research determine the feasibility of generating water plume barriers with shapes and induced forces that satisfy those values of α and β .

The work in this thesis assumes zero rudder deflection angle, no environmental disturbances such as wind, current, and no countermeasures from the SAW like steering the SAW back to its destructive course. A modeling and simulation effort is recommended to take into account non-zero rudder deflection angle, environmental disturbances, and countermeasures from the SAW in the assessment of the counter-SAW mission effectiveness. The results of this effort could influence system concepts and counter-SAW operations.

APPENDIX A. DETERMINATION OF HYDRODYNAMIC DERIVATIVES

A maneuvering prediction program (MPP1.3) is used to determine the hydrodynamic derivatives. This Window-based computer program is developed by M.G. Parsons, Department of Naval Architecture and Marine Engineering, University of Michigan [19]. It offers two main options, namely the linear evaluation for the assessment of ship course stability, turning ability and controllability and the turning prediction for the estimation of turning circle characteristics. In this thesis, only the linear evaluation is used.

1. *Input to Maneuvering Prediction Program (MPP1.3)*

The input to MPP is through a series of five windows within the menu inputs as follows:

- Project Name
- Vessel Characteristics
- Steering Characteristics
- Operating Conditions
- Water Properties

Project Name provides a location for the general identification of the project being analyzed.

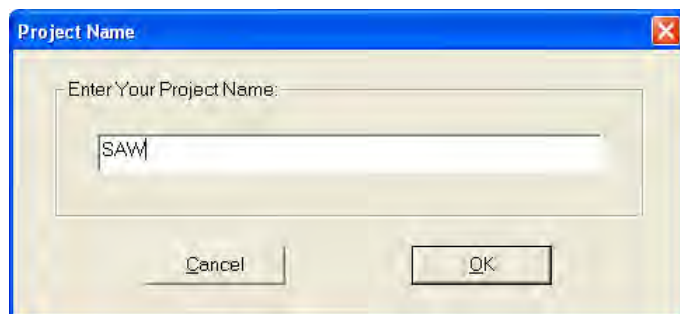


Figure 29. Input for project name

Vessel Characteristics obtains the basic dimensions, form coefficients, LCG, yaw radius of gyration, and bow profile information for the hull.

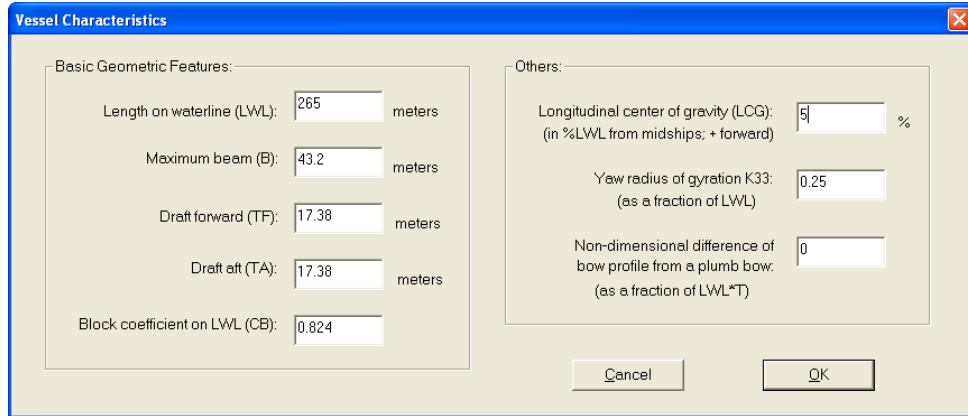


Figure 30. Input for vessel characteristics

Steering Characteristics obtains the rudder area, steering gear time constant, position of the rudder center of effort and selection of single or twin screw.

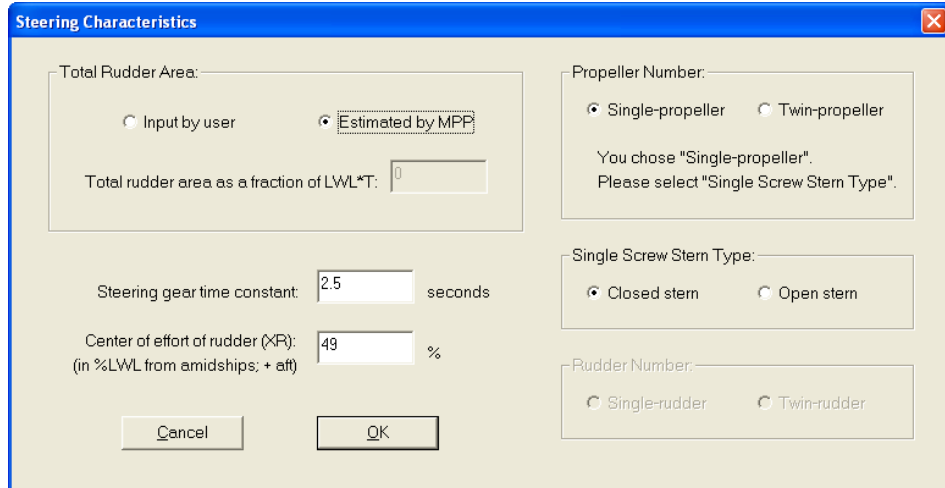


Figure 31. Input for steering characteristics

Operating Conditions obtains the water depth and the initial vessel speed.

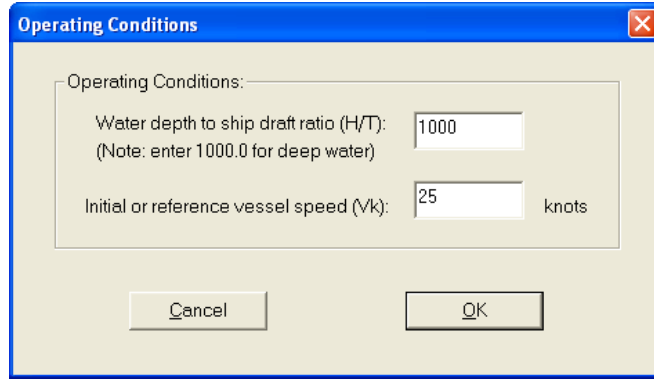


Figure 32. Input for operating conditions

Water Properties allows the choice of fresh water @ 15C, salt water @ 15C or user-specified water properties.

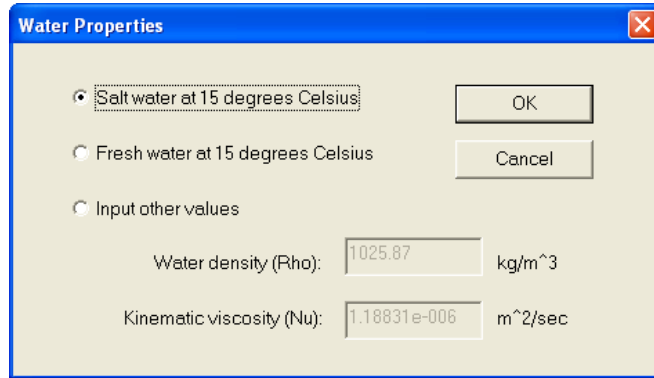


Figure 33. Input for water properties

2. *Output from Maneuvering Prediction Program (MPP1.3)*

When the input process is completed, the program can be run through the Analysis menu or by selecting the RunMPP button. This will produce a final run input window where the selection is made for the linear evaluation and there is a need to name the run identifier.

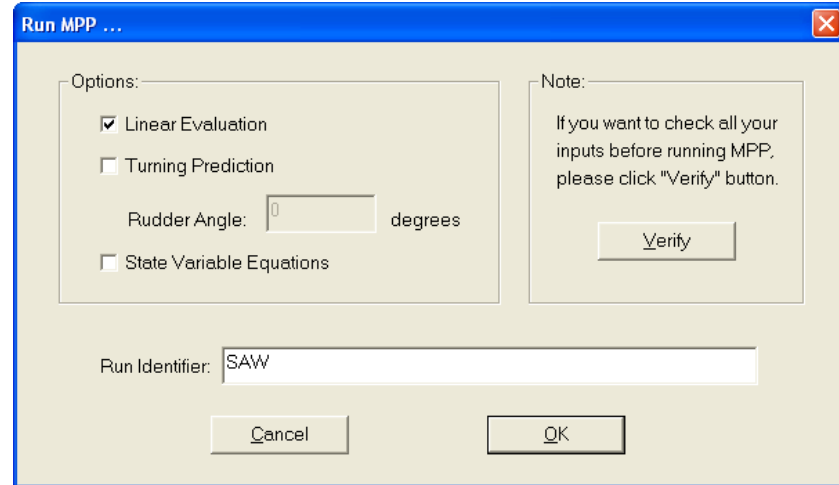


Figure 34. Input for run identifier

An output report will be generated as shown below. There is a need to check that the vessel is hydrodynamically open loop course stable in order for the values of the hydrodynamic derivatives to be usable.

Maneuvering Prediction Program - [MPP1]

File Edit View Input Analysis Window Help

University of Michigan
Department of Naval Architecture and Marine Engineering
Maneuvering Prediction Program (MPP-1.3) by M.G. Parsons

***** Linear Maneuvering Criteria Option *****

Reference: Clarke, D., Gedling, P., and Hines, G.,
"The Application of Manoeuvring Criteria in Hull
Design using Linear Theory," Trans. RINA, 1983

Run Identification: saw1

Linear Maneuvering Derivatives

Nondimensional Mass	M'	=	0.017620
Nondimensional Mass Moment	I_{zz}	=	0.001101
Sway Velocity Derivative	Y_v	=	-0.025566
Sway Acceleration Derivative	$Y_{v\dot{v}}$	=	-0.016110
Yaw Velocity Derivative	N_v	=	-0.008402
Yaw Acceleration Derivative	$N_{v\dot{v}}$	=	-0.001046
Sway Velocity Derivative	Y_r	=	0.005079
Sway Acceleration Derivative	$Y_{r\dot{v}}$	=	-0.001200
Yaw Velocity Derivative	N_r	=	-0.003691
Yaw Acceleration Derivative	$N_{r\dot{v}}$	=	-0.000870
Sway Rudder Derivative	Y_{δ}	=	0.003275
Yaw Rudder Derivative	N_{δ}	=	-0.001605

Time Constants and Gains for Nomoto's Equation

Dominant Ship Time Constant	T_1'	=	13.7685
Ship Time Constant	T_2'	=	0.3944
Numerator Time Constant	T_3'	=	0.8817
Numerator Time Constant	T_4'	=	0.2791
1st Order Eqn. Time Constant	T'	=	13.2812
Rudder Gain Factor	K'	=	-5.9580
Rudder Gain Factor	$K_{v\dot{v}}'$	=	3.0506
Steering Gear Time Constant	T_{EG}	=	0.1213

Evaluation of Turning Ability and Stability

Inverse Time Constant	$1/ T' $	=	0.0753
Inverse Gain Factor	$1/ K' $	=	0.1678
Clarke's Turning Index	P	=	0.3418
Linear Dynamic Stability Criterion	C	=	0.0000115

Vessel is hydrodynamically open loop course stable

Ready

Figure 35. Output from the Maneuvering Prediction Program (MPP1.3)

THIS PAGE INTENTIONALLY LEFT BLANK

APPENDIX B. MATLAB PROGRAM CODE

```

clear all
clc
%
%=====
% Input Variables

alpha = 0.3;      % Increase in draft, values range 0 to 1
beta = 0.3;       % Applied Fwpb @ Fwd area, values range 0 to 1
Delta = 0.;        % Set rudder deflection angle to zero

%=====
% Declarations

rho = 1025.;      % Density of seawater
g = 9.81;         % Gravitational Accelerations

L = 265.;         % Length of SAW
B = 43.2;         % Breath of SAW
T = 17.38;        % Draft of SAW

u = 12.86;        % Velocity of SAW (25knots = 12.86m/s)

%=====
% Formulations

phi = atan((T*alpha)/B);
Fwpb = -1*rho*g*L*B*0.5*((2*T)+(T*alpha))*sin(phi)*beta % Force
calculation

l = L/2-(0.15*L); % Moment Length wrt amidships
Nwpb = l*Fwpb;     % Moment calculation

Fwl = (Fwpb)/(0.5*rho*(u^2)*(L^2));      %non dimensionize
Nwl = (Nwpb)/(0.5*rho*(u^2)*(L^3));      %non dimensionize
Deltal = (Delta/180)*pi;
U = 1.;           %Assume constant forward speed & non dimensionize
xg = 0.05;

%=====
%Hydrodynamics Derivatives Values from Maneuvering Program (University
of Michigan)
m = 0.017620;
Iz = 0.001101;

Yv = -0.025566;
Yvdot = -0.016110;

Nv = -0.008402;
Nvdot = -0.001046;

```

```

Yr      =  0.005079;
Yrdot   = -0.001200;

Nr      = -0.003691;
Nrdot   = -0.000870;

Ydelta  =  0.003275;
Ndelta  = -0.001605;

Den = (Iz-Nrdot)*(m-Yvdot) - (m*xg-Yrdot)*(m*xg-Nvdot);
a11 = ((Iz-Nrdot)*Yv - (m*xg-Yrdot)*Nv)/Den;
a12 = ((Iz-Nrdot)*(Yr-m) - (m*xg-Yrdot)*(Nr-m*xg))/Den;
a21 = ((m-Yvdot)*Nv - (m*xg-Nvdot)*Yv)/Den;
a22 = ((m-Yvdot)*(Nr-m*xg) - (m*xg-Nvdot)*(Yr-m))/Den;
b1   = ((Iz-Nrdot)*Ydelta - (m*xg-Yrdot)*Ndelta)/Den;
b2   = ((m-Yvdot)*Ndelta - (m*xg-Nvdot)*Ydelta)/Den;

%=====
%
% Initialization
%
v_old   = 0.;
r_old   = 0.;
psi_old = 0.;
x0_old  = 0.;
y0_old  = 0.;
%
DeltaT  = 0.001;           % Time step increment
SimTime = 5.0;             % Simulation time
NT      = SimTime/DeltaT;  % Number of simulation steps
%
% Start simulation
%
for i=1:NT,
%
% External force
%
Fw = Fwl;
Nw = Nwl;
if (i*DeltaT) > 2.0
    Fw = 0;
    Nw = 0;
end
if (i*DeltaT) < 1.0
    Fw = 0;
    Nw = 0;
end
c1 = ((Iz-Nrdot)*Fw - (m*xg-Yrdot)*Nw)/Den;
c2 = ((m-Yvdot)*Nw - (m*xg-Nvdot)*Fw)/Den;
%
% Equations
%
psidot = r_old;

```

```

vdot    = a11*v_old + a12*r_old + b1*Delta1 + c1;
rdot    = a21*v_old + a22*r_old + b2*Delta1 + c2;
x0dot  = (U*cos(psi_old)) - (v_old*sin(psi_old));
y0dot  = (U*sin(psi_old)) +( v_old*cos(psi_old));
%
% First order integration (Euler - explicit)
%
psi_new = psi_old + DeltaT*psidot;
v_new   = v_old + DeltaT*vdot;
r_new   = r_old + DeltaT*rdot;
x0_new  = x0_old + DeltaT*x0dot*u;
y0_new  = y0_old + DeltaT*y0dot*u;
ang_old = 0;
ang_new = ang_old + (atan(abs(y0_new)/x0_new))*57.2958;
%
% Store results
%
psi(i)      = psi_new;
psidot_v(i) = psidot;
v(i)        = v_new;
vdot_v(i)   = vdot;
r(i)        = r_new;
rdot_v(i)   = rdot;
x0(i)       = x0_new;
y0(i)       = y0_new;
Fw_v(i)     = Fw;
Nw_v(i)     = Nw;
time(i)     = i*DeltaT;
angle(i)    = ang_new;
%
% Update state vector x for the next simulation step
%
psi_old = psi_new;
v_old   = v_new;
r_old   = r_new;
x0_old  = x0_new;
y0_old  = y0_new;
end
%
% Plotting of graphs
%
figure(1)
plot(time,psi*57.2958); xlabel('t (sec)'); ylabel('psi (deg)'); grid
%
figure(2)
plot(time,v); xlabel('t (sec)'); ylabel('v'); grid
%
figure(3)
plot(time,r); xlabel('t (sec)'); ylabel('r'); grid
%
figure(4)
plot(time,psidot_v); xlabel('t (sec)'); ylabel('(d/dt)\psi'); grid
%
figure(5)
plot(time,vdot_v); xlabel('t (sec)'); ylabel('(d/dt)v'); grid

```

```

%
figure(6)
plot(time,rdot_v); xlabel('t (sec)'); ylabel('( $d/dt$ )r'); grid
%
figure(7)
plot(time,Fw_v); xlabel('t (sec)'); ylabel('Fw'); grid
%
figure(8)
plot(time,Nw_v); xlabel('t (sec)'); ylabel('Nw'); grid
%
figure(9)
plot(x0,y0); xlabel('x'); ylabel('y'); grid
title ('x0 vs y0 (Dimensional)')
%legend('Force #1','Force #2','Force #3','Force #4','location','best');
%
figure(10)
plot(time,angle,'b-'); xlabel('t (sec)'); ylabel('deg'); grid
title ('Time vs Angle of Deflection (Dimensional)')
%legend('Force #1','Force #2','Force #3','Force #4','location','best');

```

LIST OF REFERENCES

- [1] Reuters, “Maritime Terrorism: What are the risks?,” March 2010, <http://blogs.reuters.com/andrew-marshall/2010/03/05/maritime-terrorism-what-are-the-risks/> [Accessed on 11 Oct 2011]
- [2] Paul W. Parfomak and John Frittelli, “Maritime Security: Potential Terrorist Attacks and Protection Priorities,” Congressional Research Service, RL33787, May 2007.
- [3] Systems Engineering and Analysis Cohort Seven, “Maritime Domain Protection in the Straits of Malacca,” Thesis Technical Report, Naval Postgraduate School, Monterey, CA, United States, NPS-97-05-001, 2005.
- [4] US Energy Information Administration, “World Oil Transit Chokepoints,” February 2011, <http://www.eia.gov/countries/regions-topics.cfm?fips=WOTC> [Accessed on 11th Oct 2011]
- [5] Wikipedia, “Straits of Johor,” November 2011, http://en.wikipedia.org/wiki/Strait_of_Johor [Accessed on 11 Oct 2011]
- [6] Wikipedia, “Sea state,” November 2011, http://en.wikipedia.org/wiki/Sea_state [Accessed on 11 Oct 2011]
- [7] P. Tkalich, Pang W.C., and P. Sundarambal, “Hydrodynamics and Eutrophication Modelling for Singapore Straits,” in *The Seventh OMISAR Workshop on Ocean Models*, 2002, p. 5–4.
- [8] Wikipedia, “Geography of Singapore,” November 2011, http://en.wikipedia.org/wiki/Geography_of_Singapore#cite_note-3 [Accessed on 11th Oct 2011]
- [9] WEATHERWise Singapore, National Environment Agency, Singapore, 2009, p. 12.
- [10] Chia Lin Sien, “The Importance of the Straits of Malacca and Singapore,” *Singapore Journal of International & Comparative Laws*, 1998, p. 302.
- [11] Jurong Island Factsheet 2011, Singapore Economic Development Board, Singapore, 2011.
- [12] Singapore Economic Development Board, “Industry Background,” March 2011, http://www.sedb.com/edb/singapore/index/industry_sectors/energy/industry_background.html [Accessed on 11 Oct 2011]
- [13] Maritime and Port Authority of Singapore (MPA), “Operational Areas,” 2009, [http://www.mpa.gov.sg/sites/port_and_shipping/port/vessel_traffic_information_system\(vtis\)/straitrep/operational_areas.page](http://www.mpa.gov.sg/sites/port_and_shipping/port/vessel_traffic_information_system(vtis)/straitrep/operational_areas.page) [Accessed on 11 Oct 2011]
- [14] Adrian Biran, *Ship Hydrostatics and Stability*. Butterworth Heinemann, 2003.

- [15] xVAS, “vessel assessment system,”
<http://www.xvas.it/SPECIAL/VTship.php?imo=8809919&mode=CK> [Accessed on 11 Oct 2011]
- [16] Global Security, “Shipboard Measurements,” July 2011,
<http://www.globalsecurity.org/military/systems/ship/measurement.htm> [Accessed on 11 Oct 2011]
- [17] D. My-Ha, K.M. Lim, B.C. Khoo, K. Willcox, “Real-time optimization using proper orthogonal decomposition: Free surface shape prediction due to underwater bubble dynamics,” *Computers & Fluids*, vol 36, pp. 499–512, March 2007.
- [18] “Dynamics of Marine Vehicles,” Informal Lecture Notes for ME 4823, Department of Mechanical Engineering, Naval Postgraduate School, Summer 1993.
- [19] M. G. Parsons, “Maneuvering Prediction Program (MPP1.3),” Windows based computer program, December 1994.

INITIAL DISTRIBUTION LIST

1. Defense Technical Information Center
Ft. Belvoir, Virginia
2. Dudley Knox Library
Naval Postgraduate School
Monterey, California
3. Fotis A. Papoulias, PhD
Department of Mechanical and Aerospace Engineering
Naval Postgraduate School
Monterey, California
4. Thomas V. Huynh, PhD
Department of Systems Engineering
Naval Postgraduate School
Monterey, California
5. Khoo Boo Cheong, PhD
Department of Mechanical and Aerospace Engineering
National University of Singapore
Singapore
6. Yeo Tat Soon, Director
Temasek Defence Systems Institute
Singapore
7. Leo Tin Boon, Senior Associate Director
Temasek Defence Systems Institute
Singapore
8. Tan Lai Poh, Manager
Temasek Defence Systems Institute
Singapore